Carderock Division
Naval Surface Warfare Center
West Bethesda, MD 20817-5700

CARDIVNSWC-TR–61-99/28 1999

Survivability, Structures and Materials Directorate
Technical Report

Characterization of the Surface Film Growth During the Electrochemical Process; Part I: Nickel - Sea Water System

by
A. Srinivasa Rao

CARDIVNSWC-TR–61-99-28 Characterization of the Surface Film Growth During the Electrochemical Process: Part I Nickel - Sea Water System

Carderock Division
Naval Surface Warfare Center
West Bethesda, MD 20817-5700

CARDIVNSWC-TR–61-99/28 1999

Survivability, Structures and Materials Directorate
Technical Report

Characterization of the Surface Film Growth During the Electrochemical Process; Part I: Nickel - Sea Water System

by
A. Srinivasa Rao

REPORT DOCUMENTATION PAGE

Form Approved
OMB No. 0704-0188

1. AGENCY USE ONLY (Leave blank)	2. REPORT DATE	3. REPORT TYPE AND DATES COVERED
	June 1998	Research and Development

4. TITLE AND SUBTITLE
Characterization of the Surface Film Growth During the Electrochemical Process: Part I Nickel – Sea Water System

5. FUNDING NUMBERS
98-1-6120-650

6. AUTHOR(S)
A. Srinivasa Rao

7. PERFORMING ORGANIZATION NAME(S) AND ADDRESS(ES)
Carderock Division
Naval Surface Warfare Center
Bethesda, MD 20817-5000

8. PERFORMING ORGANIZATION REPORT NUMBER
CARDIVNSWC-TR- 61-99-28

9. SPONSORING/MONITORING AGENCY NAME(S) AND ADDRESS(ES)

10. SPONSORING/MONITORING AGENCY REPORT NUMBER

11. SUPPLEMENTARY NOTES

12a. DISTRIBUTION/AVAILABILITY STATEMENT
Distribution unlimited. Approved for public release

12b. DISTRIBUTION CODE

13. ABSTRACT (Maximum 200 words)

In order to understand the resistance of passive films formed during corrosion processes, an analytical technique using x-ray diffraction was developed to examine the structure of metal in closest proximity to the metal / liquid interface. The in-situ structure at the metal liquid interface was examined for pure nickel in sea water solution at room temperature and at two different potentistatically controlled potentials (- 800 mV and + 450 mV versus Ni/NiO). The chemical changes at the metal interface were studied over a period of 72 hours. The x-ray diffraction results indicated that the structure of both the inner and the outer passive layers, at – 800 mV (versus Ni/NiO), is comprised of both $Ni(OH)_2$ and γ - NiOOH. Similarly the structure of the the interfaces at + 450 mV (versus Ni/NiO) contains both NiO and Ni_2O_3. XPS analysis of the surface structure (primarily of the outer passive layer) suggests that at – 800 mV (versus Ni/NiO) the structure consists of nearly 100 % $Ni(OH)_2$. The structure at + 450 mV (versus Ni/NiO) consists of nearly 90 % Ni_2O_3 and 10 % $Ni(OH)_2$. It is therefore possible that the structure of inner passive layer is γ - NiOOH at – 800 mV and $Ni(OH)_2$ at + 450 mV.

14. SUBJECT TERMS

15. NUMBER OF PAGES

16. PRICE CODE

17. SECURITY CLASSIFICATION OF REPORT	18. SECURITY CLASSIFICATION OF THIS PAGE	19. SECURITY CLASSIFICATION OF ABSTRACT	20. LIMITATION OF ABSTRACT
Unclassified	Unclassified	Unclassified	Unclassified

CONTENTS

FIGURES

Page No.

ABSTRACT

In order to understand the resistance of passive films formed during corrosion processes, an analytical technique using x-ray diffraction was developed to examine the structure of metal in closest proximity to the metal / liquid interface. The in-situ structure at the metal liquid interface was examined for pure nickel in sea water solution at room temperature and at two different potentistatically controlled potentials (- 800 mV and + 450 mV versus Ni/NiO). The chemical changes at the metal interface were studied over a period of 72 hours. The x-ray diffraction results indicated that the structure of both the inner and the outer passive layers, at – 800 mV (versus Ni/NiO), is comprised of both $Ni(OH)_2$ and γ - NiOOH. Similarly the structure of the the interfaces at + 450 mV (versus Ni/NiO) contains both NiO and Ni_2O_3. XPS analysis of the surface structure (primarily of the outer passive layer) suggests that at – 800 mV (versus Ni/NiO) the structure consists of nearly 100 % $Ni(OH)_2$. The structure at + 450 mV (versus Ni/NiO) consists of nearly 90 % Ni_2O_3 and 10 % $Ni(OH)_2$. It is therefore possible that the structure of inner passive layer is γ - NiOOH at – 800 mV and $Ni(OH)_2$ at + 450 mV.

ADMINSTRATIVE INFORMATION

This report, covering the research work for the period of FY 99, was funded by the NSWC CD Independent Research Program (ILIR), sponsored by the Office of the Naval Research, ONR10, and administered by the Research Director, NSWC CD 0112, Dr. Bruce Douglas, under the program element 61152N, Task Area ZR-000-01-0I and the NSWC CDWork Unit 1 - 6120 - 650. This work was supervised within the Metals Department (Code 61) by Dr. L. F. Aprigliano (Code.612).

INTRODUCTION

BACKGROUND

The development of new materials with improved hot water and salt-water corrosion resistance is very important. As these materials are being proven, it is also important to develop procedures and methods to maintain the existing materials currently in use. Technologically advanced maintenance procedures would have applications in several areas, viz. electric utilities for the removal of deposits from thermal power plant equipment, and in the civilian and military ship building industry for the removal of corrosion products from ship platforms and on-board tanks. Reductions in military and industrial acquisition budgets have led to reduced new equipment purchases. Therefore, the need has increased to extend the operational life of the current systems. In addition, the environmental constraints on materials selection and maintenance processes are increasingly becoming a major concern in utility plant operation and maintenance.

A key to the extension of equipment life is the reduction of material degradation/ failure rates. The degradation rates of both naval and electrical utility systems are exacerbated by salt water and hot corrosion. The lessons learned to control the corrosion in one system can be used to the benefit of another. The use of thin films, e.g. oxides, has been the first line of defense in protecting machinery systems from the onset of corrosion. When these films are passive to the environment, they can impart excellent corrosion resistance. A fundamental, electrochemical understanding of how passive films resist

the effects of corrodants will provide a means to improve the life of machinery components.

Saltwater and hot corrosion processes are controlled by the chemical reactions that take place at the metal/liquid interface. In general, this is often studied with analytical techniques that look through the liquid to see the interface. Although it is more difficult, it may be far more revealing to view this interface by looking at it from the other side - through the metal. By doing this, new information can be gained concerning the manner in which a passive film resists the action of a liquid corrodant. This information can then be used to design more protective films in systems that are not normally passive. The passive film formation process involves the transformation of a metal into a undesirable compound. If one is to interrupt this process, it is useful to know if the final compound is preceded by the meaningful formation of an intermediate compound.

In the recent past, a number of in-situ and structure sensitive studies were made of electrochemical processes within the confines of conventional and ultra high vacuum (uhv) systems. [1-3]. Most of these earlier studies involved the emission and or the scattering of photons or charged particles as a part of the analysis technique. These techniques could provide only indirect information regarding the structure of the corrosion products and interfaces. In the open literature, there have been reports on the elucidation of structure during electrochemical processing using neutron diffraction [4]. However, the neutron diffraction studies required an elaborate and complex experimental set up. Of late, a few investigators have suggested the feasibility of experiments using analytical techniques such as the surface extended x-ray adsorption fine structure

(SEXAFS), x-ray adsorption near edge structure (XANES), and total external reflection Bragg diffraction (TRBD) [5-8]. However, these studies often ignored the near-metal side of the metal/liquid interface, because the extent of the reaction product is so much broader on the liquid side than the metal side (1-10 μm versus 1-20 nm) of the metal/liquid interface.

NICKEL / NICKEL ALLOY SYSTEM

The electrochemistry of nickel and nickel alloy systems warrants study by the scientific community because these systems are pertinent to many utility and naval machinery components. During corrosion, nickel and its alloys undergo the formation of passive oxyhydrates and/or hydroxides. In the literature it has been reported that the identification of the formation of nickel hydroxides and or oxyhydrates has been difficult because these compounds often have highly disordered and/or have an amorphous crystal structure. Several earlier researchers used analytical techniques such as the EXAFS [5-6] and XAS [7-9] to study nickel compounds. However, these researchers focussed their attention on understanding the oxidation state of the nickel (Ni^{4+}) during the electrochemical process instead of examining the nucleation and growth of new compositions at the interface.

Except for our earlier study of the interface of nickel, copper - nickel in KOH solution [10 – 12], only two other investigators [13,14] have focussed their attention on understanding the structure of the near metal side of the metal liquid interface.

In one [13], it was reported that the in-situ x-ray diffraction study is the key to understanding the electrochemical processes at the nickel electrode solution interface. These researchers designed and developed an electrochemical cell for x-ray reflection mode experiments. They reported that they found a 0.75 μm thick layer of $Ni(OH)_2$ after 40 hours of chemical reaction of nickel in 5 M KOH at 1 mV/sec. However, their x-ray diffraction data showed very broad peaks. They concluded that the broadening was due to a mixture of phases in incompletely aged electrodes.

Another in-situ x-ray diffraction analysis [14,15] involved the study of the structure of nickel electrodes during hydrogen evolution in sulfuric acid electrolysis. Those investigators reported that by x-ray diffraction they observed the formation of β-NiH. They have also reported that they resolved the structure of β-NiH by x-ray diffraction. The peaks were very sharp and the 2θ values corresponding to β-NiH (111),(200) and (220) were at 41.9, 48.8 and 71.1 degrees respectively.

PASSIVE LAYER DEGRADATION

The passive oxide films/ layers on many corrosion resistant alloys (e.g. stainless steels and copper/nickel alloys) are what distinguish them from alloys that readily corrode in aqueous environments. However, even these alloys can corrode and their passive layers degrade in many industrial applications. The mechanism of passive layer degradation has been extensively studied from the perspective of the aqueous side of the process. It has not been extensively studied from the perspective of the metal side of the

process, due to the complexity of the interface region. As the electrochemical reaction starts, at the interface, the metal will be converted to its corresponding oxide. This oxide layer then may act as a passive barrier, thus retarding progression of the electrochemical process. The intriguing question is whether the passive film extends from the solution to the reacting interface of the metal and or whether it forms another transient inner passive layer? Assuming that such a process exists, the electrochemical process can be represented schematically as follows. Figure 1 shows a schematic diagram of the metal - solution interface region during an electrochemical reaction process. The metal interface region can be divided into possibly four regions: (a) bulk metal, (b) inner passive layer, (c) outer passive layer and (d) solution. The existence of an inner passive layer (nano meters (10 - 20 nm) thick) has widely been accepted by the scientific community. Most of the earlier conventional studies have studied the degradation of the passive layers by observing the interface region from the solution side (Figure 1(A)). The proposed, present approach will be to investigate the structure of the inner passive layer from the metal side of the metal solution interface (as shown in Figure 1(B)). The motivation to the present approach is the desire to establish the nucleation and growth of inner passive layer and to detect the passive layer structure in-situ by the present experimental analytical technique.

OBJECTIVES

The present investigation was conceived to conduct a systematic study of the near metal interface structure in nickel/nickel oxide system during the alkaline (sea water) hydrolysis. The overall goals of this program are (1) to develop an experimental method to ascertain basic scientific information of the chemical and electrochemical interactions at the near metal - chemical reagent interface during electrochemical process, and (2) to

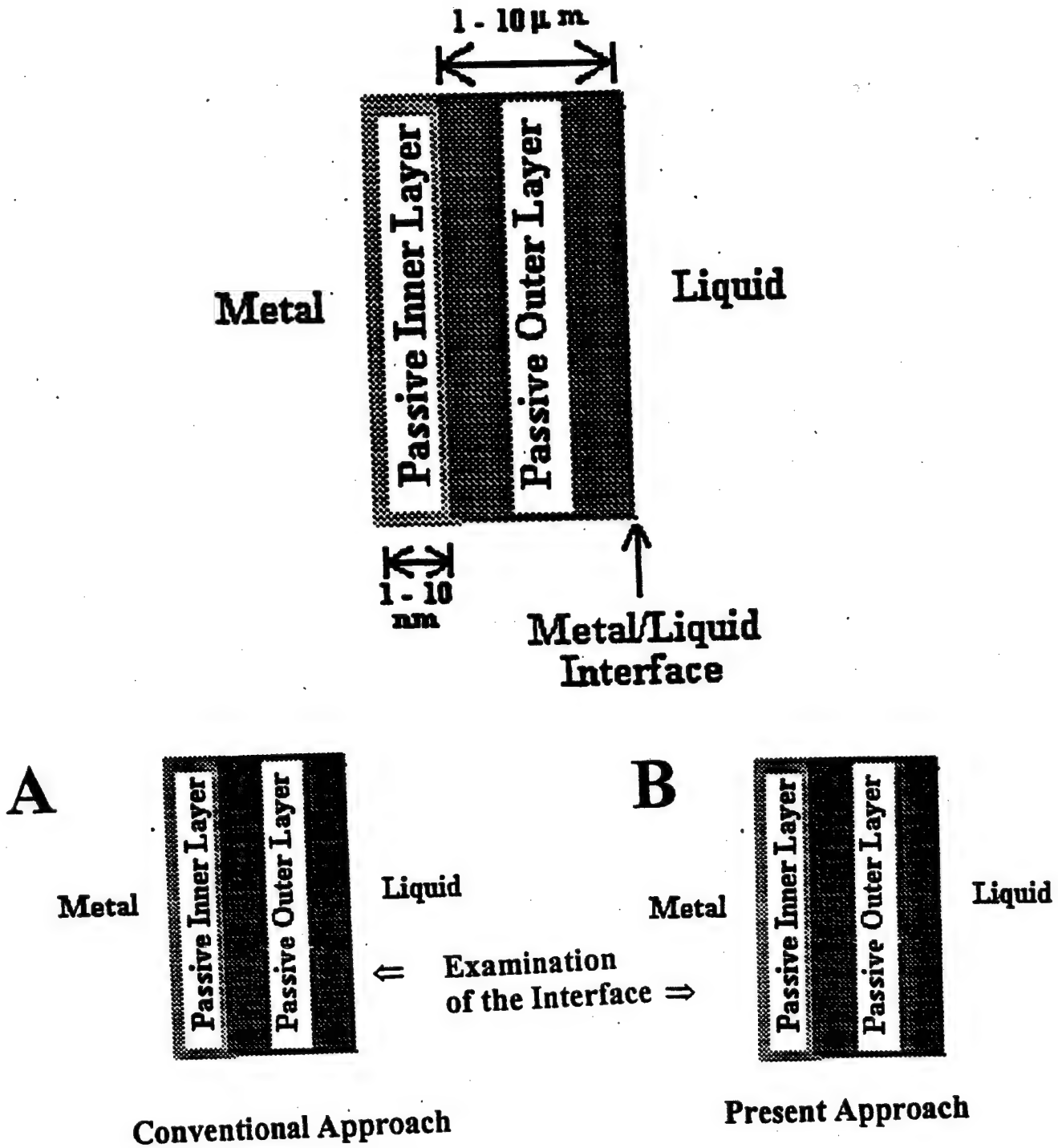

Figure 1. Schematic diagram of the metal/solution interface region during electrochemical reaction process. (A) Conventional and (B) present approach to study the inner passive layer.

characterize the changes in the composition of nickel alloy materials. Consequently, the objectives of this investigation can be summarized as follows:

1. To develop an analytical method to study the reaction of metal/liquid interfaces from the metal side.
2. To apply this method to study reactions at an established, and simplified metal/corrodant interface, i.e. nickel/sea water.
3. To apply this method to a more complicated metal alloy system, e.g. 90/10 and/or 70/30 Cu/Ni, and stainless steels.

EXPERIMENTAL PROCEDURE

As part of the first phase of this project an experimental electrochemical cell was designed, fabricated, and tested. This cell was designed to allow for the use of x-ray diffraction as a method to study the corrosion process from the metal side of the metal/liquid interface. In that first phase of our work, the nickel – sea water interface was studied in conjunction with the electrochemical characteristics of the corrosion process in the cell.

MATERIALS

Commercial grade (of 99.99 % purity) nickel foil was used during this investigation. The as – received foil has an average thickness of 12.5 μm (0.0005"). The foil surface was cleaned with acetone and alcohol to remove any residual surface impurities. A simulated sea water solution was used during the present investigation. It

was prepared according to the ASTM Standard. The further use of the term sea water in this report relates to the use of simulated and not actual sea water.

ELECTROCHEMICAL CELL DESIGN

Figure (2 (A)) shows the schematic diagram of an electrochemical cell reported in the open literature for in-situ examination of the changes in the structure of the interface region. The principle behind the cell design is the application of Bragg configured reflection mode x-ray measurement of the interface. The design incorporates a window with a complex arrangement for the placement of a thin metal foil facing the incoming x-ray source. The x-ray beam is transmitted through the foil and diffracted to a detection system. Although this type of cell arrangement can provide satisfactory information, the resolution can be poor. It is because the angle between the incident and reflected x-ray beam is small. As a result, interference between the incident and reflected x-rays increases, and such an increase in interference decreases the resolution. The second disadvantage is that the above cell design requires a complex metal foil assembly.

In this investigation an x-ray diffraction unit in which the detector system moves vertical to the plane of the sample foil and the x-ray source was used. This was done to increase the angle between the incident and reflected x-ray beam and to maximize the uninterferred Bragg reflection. Additionally, a new cell was designed for ease of metal foil mounting.

Figure 2(B) shows a schematic diagram of the electrochemical cell. It was designed to be easily attached to and detached from the x-ray unit. A noteworthy feature of this cell design is that the top surface of the electrochemical cell was kept at an

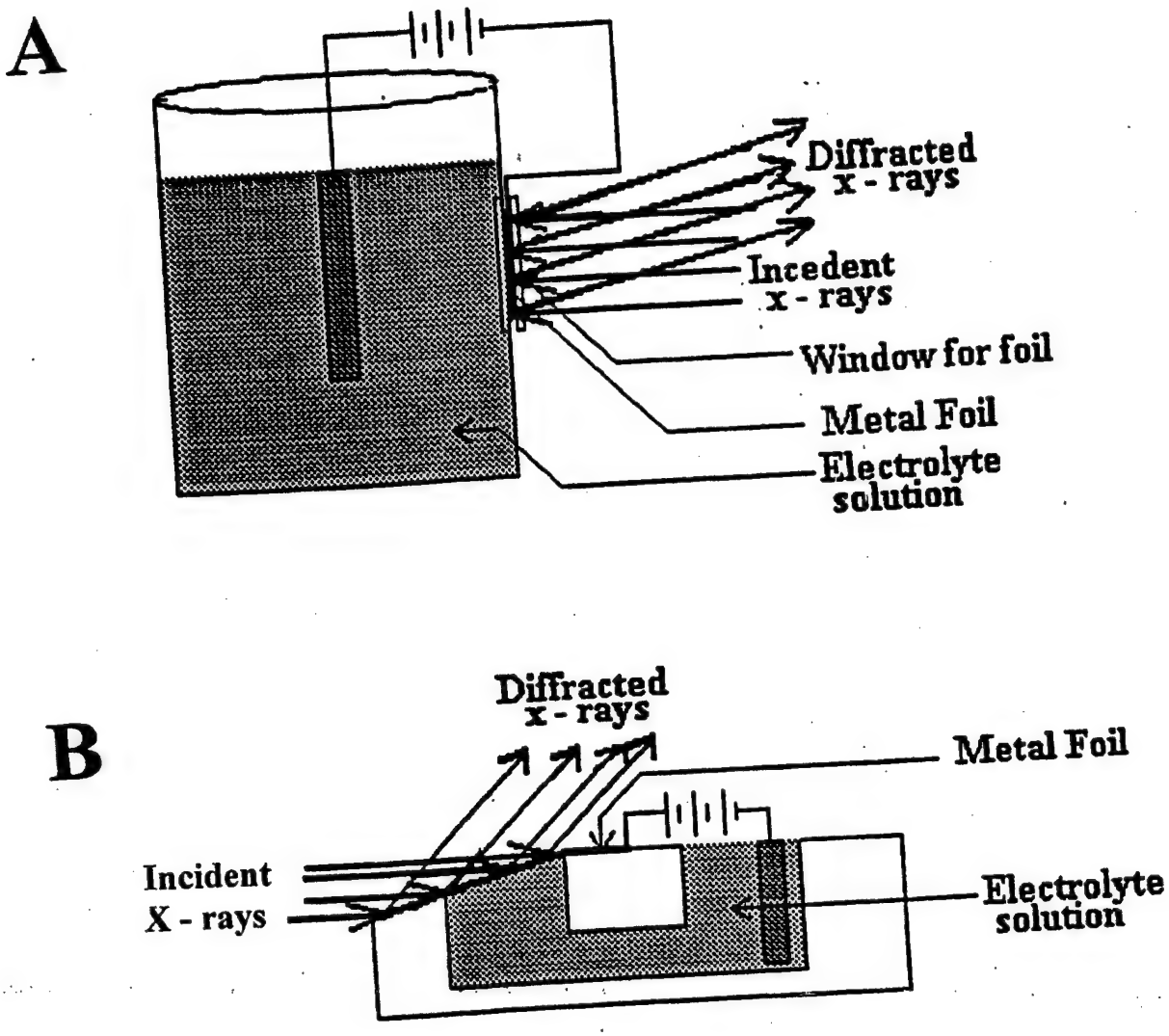

Figure 2. Schematic diagram of the design of the electrochemical cell (A) reported in the literature and (B) designed during this investigation.

inclined angle of 5° to the plane of the x-ray beam. At the mid point of the cell width, the cell surface is in plane with the incident x-rays The inclination of the cell surface provides for strong and sharp Bragg reflections, thus resolving sharp x-ray peaks. The need for the 5° inclination of the top surface of the cell was discovered by a process of trial and error and the detailed design specifications were given in our earlier reports (10 - 12).

ELECTROCHEMICAL PARAMETERS

In order to establish electrochemical parameters prior to the actual current density versus potential (versus reference potential) measurements, a reference nickel/nickel oxide (Ni/NiO) electrode system was fabricated based on the electrochemical cell design specifications. While the electrode designing and dimensional requirements were developed by us, the actual electrode construction was done by E-TEK Inc., Natick, MA. The nickel/nickel oxide (Ni/NiO) electrode was constructed on a 80X80 nickel mesh screen consisting of a screen flag 2.5 x 1 cm with a connection piece 10 cm long. The Ni/NiO system was produced as a Ni/NiO/PTFE electrode. The final form of the electrode is a basket with 0.8 cm diameter x 1 cm depth.

The Ni/NiO/PTFE electrode was placed in a beaker consisting of simulated sea water solution. Nickel strips were used as the other electrodes of the electrochemical cell. The electrodes were connected to a computer controlled potentiostatic analyzer. The analyzer system consists of a Princeton Applied Research (PAR) PARC Model 273 potentiostat, and an EG&G 5206 Lock-in Amplifier with a conventional PC, utilizing the PARC M 388 Software for system control and data accumulation.

X-RAY DIFFRACTION PARAMETERS

A Sintag XDS-2000 x-ray diffractometer with a CuKα1 source at 8048 eV, 2.5 FWHM was used during this investigation.

The x-ray energy, current and the foil thickness were 35 KV, 30 mA and 12.5 μm (0.0005") respectively.

TEST PROCEDURE

The test cell was filled with the simulated sea water solution that was pre-electrolyzed in order to remove any cationic impurities. Due care was taken during the filling of the test cell to ensure that no air bubbles were trapped between the nickel foil and the solution. The test cell was attached to the x-ray unit and the electrochemical testing was initiated. In order to maximize the electrochemical (cathodic and anodic) reaction, the critical electrode potentials were determined using cyclic voltametry. For nickel / sea water system it was found that at – 800 mV and + 450 mV, the electrochemical reaction is at its maximum. Therefore, two pre-selected constant potentials (- 800 mV or + 450 mV) were applied continuously during each electrochemical study period of nearly 72 hours.

In order to follow the structural changes during the electrochemical process, x-ray diffraction patterns were obtained without any potential, and after 1, 2, 4, 6 and 24 hours. Each x-ray diffraction run took 20 minutes. For convenience, we have labeled the x-ray diffraction patterns as those obtained after 1, 2, 4, 6 and 24 hours only.

X-RAY PHOTOELECTRON SPECTROSCOPY (XPS)

X-ray photoelectron spectroscopy (XPS) was used to examine the nature of the surface reactions that were the subject of this research effort. It was also used to study the nature of the initial oxides formed on the test foils. XPS involves exposing the surface of interest to x-rays of a discrete energy. In the Kratos model XSAM 800 surface analyzer used in these experiments, AlKα (1486.6 eV, 1 FWHM) was the radiation source. This radiation interacts with the specimen, causing the material to emit electrons whose-energy is characteristic of the atoms from which they were emitted. The XPS equipment has an electron energy analyzer, which measures the kinetic energy of the emitted electrons. This measurement is made with a hemispherical analyzer having an aberration-compensated input lens (ACIL). The analyzer superimposes different voltages on the inner and outer hemispheres, which then allow only electrons with energies between these two values to pass through to the detector at the opposite end of the analyzer. The equipment scans the voltages on the two hemispheres through an energy range in steps, and during its dwell time at each step it keeps track of the counts per second, or intensity of electrons. This information can then be graphed as electron energy versus intensity. The major limit on the energy-resolving capabilities of the instrument is the width of the exciting radiation, e.g. 1.0 eV at full-width half maximum for Al Kα.

The XPS spectrometer and specimen are contained within an ultra-high vacuum. This prevents the electrons from being scattered by gas molecules before they reach the analyzer and allows experiments to be conducted and data acquired in reasonable times before the specimen surfaces are excessively contaminated with unwanted gases and carbon from the atmosphere. This latter point is important since the XPS method

analyzes for elements on the surface and within only several atomic layers of the surface. The surface sensitivity of the XPS method arises from its ability to measure the energy of emitted electrons. These electrons have a very short mean free path in solid matter. Typically, this distance is on the order of 5 to 10 angstroms. Therefore, the emitted electrons represent elements present in the outer layer or several atomic layers below the surface.

The concentration of a given element in the surface is represented by the intensity of electrons (counts per second) emitted at a given characteristic energy. The area under these peaks in the XPS spectrum is used as a measure of the intensity. Computer-aided routines are used to perform the necessary background subtraction around the peak of interest and to calculate the area under the peak. If peaks partially overlap, a peak synthesis routine is used to extract the peak of interest. All intensities are then corrected by a multiplication factor, which represents the spectrometer efficiency and the probability of emission from a particular electron energy level in a given atom. These correction factors were determined by the analyzer's manufacturer. To assist in identifying the chemical state of the metal foils after corrosion testing, XPS spectra were made of standards of pure nickel. The nickel foil may have an oxide layer that is nonconductive and charge up during the spectra acquisition. This can cause the peaks to shift from the normal locations. To correct for this, the adventitious carbon peak found on these standards was referenced to the carbon peak at 284.6 eV and all other peak locations were corrected accordingly. In the case of the partially overlapping peaks, a peak synthesis routine was used to separate and identify each contribution.

The details of the analysis parameters used to acquire the XPS data are :

- Al excitation (1486.6 eV)
- Fixed analyzer transmission
- True time averaging
- Low magnification
- Start energy of scan, 1200 eV
- Step size, 0.5 eV
- Low resolution
- Channels, 2400
- Dwell, 0.5 s.

The experimental procedure adopted for obtaining the XPS spectrum and for the spectral analysis is as follows: First, a sample surface analysis survey scan in the binding energy range 0 – 1200 eV was made in order to ensure that all the relevant elements are identifiable. A series of regional scans for required elements (viz. Cu, Ni, O and C) was made. The range of the scan was within $\pm$ 10 eV of the corresponding binding energy. In order to minimize any chemical changes that may result due to surface heating, prior to the acquisition of the XPS spectra, no sputter cleaning of the surface was made. This is because sputter cleaning may induce some chemical changes (viz. oxidation) due to local heating

In order to obtain the maximum information for all elements at a minimum time, only one energy sweep per element was made. Once the XPS spectra was obtained, a peak synthesis routine was used to match real data peaks / curves of interest.

INTERFACE STRUCTURE IDENTIFICATION PROCEDURE

For the foil thickness used in this investigation, it is reasonable to suggest that the x-ray diffraction patterns represent the cumulative structure of metal and the metal/liquid

interface. Since the interface region is composed of both the inner passive layer and the outer passive layer, it is reasonable to assign the x-ray diffraction data to represent the structure of the base metal and the inner and outer passive layers.

The information acquired in the XPS data represents the structure of the top few layers of the electrochemically reacted surface. Since the top few layers are contained in the outer passive layer (Figure 1), the XPS analysis can be suggested to provide information on the outer passive layer without being obscured with the information from the inner passive layer or the bulk material. By subtracting the structure of the outer passive layer (obtained from XPS data) from the XRD structural information, the inner passive layer structure can be established.

Following the verification and testing of the electrochemical cell and foil parameters two types of experiments were performed (the electrochemical property parameter study using cyclic voltametry and the chemical compositional studies). While the cyclic voltametry was done using a potentistat, the compositional studies were made using x-ray diffraction and XPS analysis (as a function of applied corrosion current).

RESULTS

NICKEL - SEA WATER SYSTEM

Figure 3 shows a typical x-ray diffraction pattern obtained from a 12.5 μm (0.0005") thick nickel foil mounted on the test cell. In order to eliminate any interference to the diffraction pattern from the cell material (lucite), the x-ray measurement program was modified to eliminate the background information on the final x-ray diffraction pattern. For example, Figure 4 shows a typical x-ray diffraction pattern obtained from the

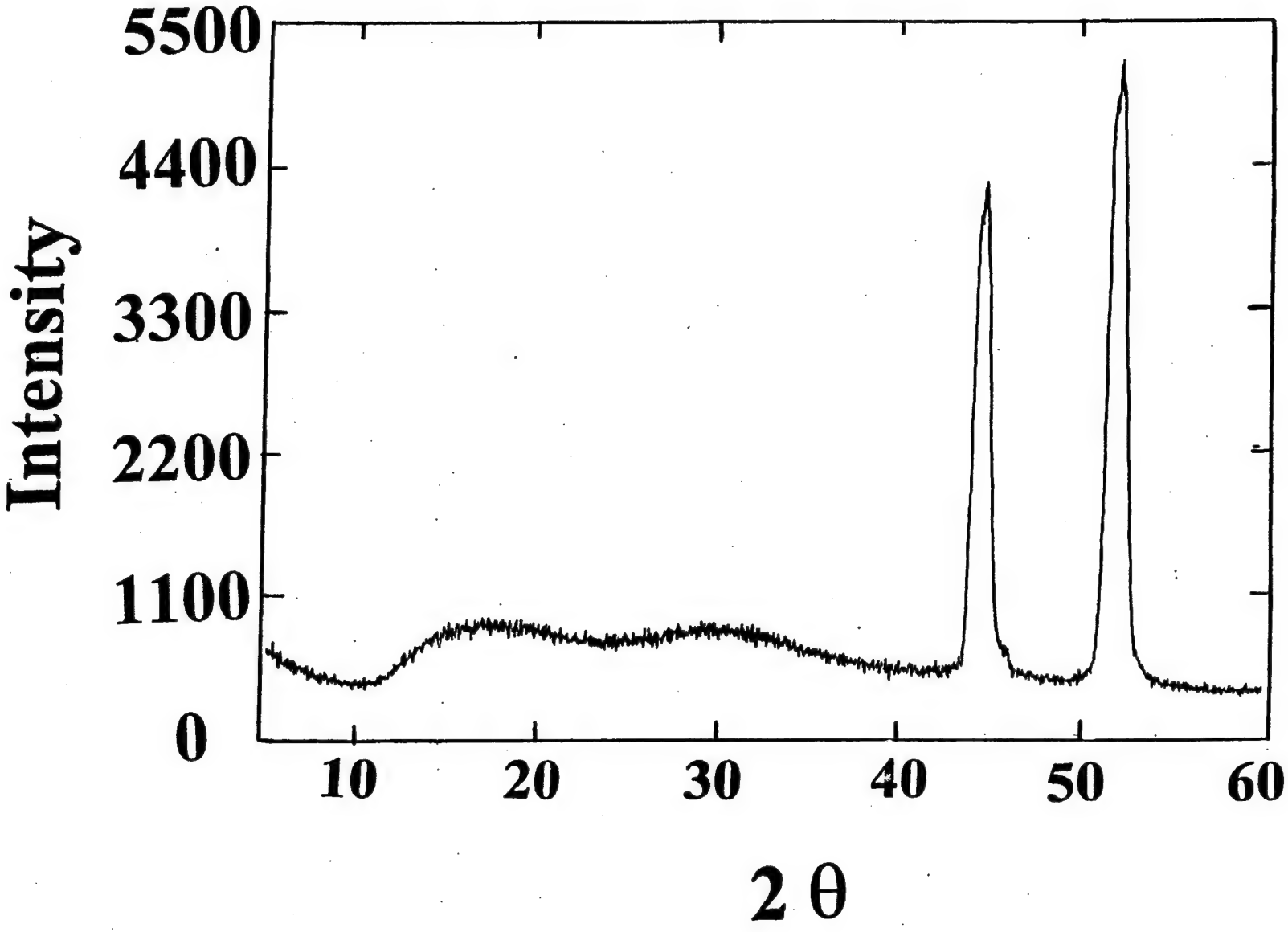

Figure 3. Typical x-ray diffraction pattern obtained from nickel foil mounted on the electrochemical test cell.

test cell material. Figure 5 shows the x-ray diffraction pattern of nickel foil shown in Figure 3 wherein the contribution due to the cell material (lucite) was removed.

Figures 6 shows a typical x-ray diffraction pattern obtained from 12.5 μm (0.0005") thick nickel foil. The two major diffraction peaks in Figures 6 correspond to the two standard diffraction peaks ($2\theta \rightarrow 44.6$ and 51.9; d spacing of 20.3 and 17.6 nm respectively). Some of the nickel samples whose grain orientation is perpendicular to the incident x-ray beam also showed an additional peak (at $2\theta \sim 41$ corresponding to d-spacing of 23 nm).

In order to make sure that the samples were thin enough to resolve the structure of the under-side of the metal foil, a calibration was carried out with a second foil. This was done with a 12.5 μm (0.0005") thick nickel foil glued onto a silver foil. The sandwich of nickel and silver foils was then glued onto the test cell. The direct exposure of silver foil to the incident x-ray beam was avoided by covering the edges with a copper shielding plate. Figure 7 shows a typical x-ray diffraction pattern of nickel/silver laminate. The silver peaks in the results demonstrate that at the x-ray incident energy studied, the x-ray penetrated through the nickel foil and into the silver foil.

The final optimized x-ray energy, current and the foil thickness (for the x-rays to penetrate through the test foil surface that is exposed to the test solution prior to the x-ray reflection to the detector system) were 35 KV, 30 mA and 12.5 μm (0.0005") respectively.

Figure 8 shows a typical current versus applied potential plot of nickel foil in simulated sea water solution as it cycles once through from – 1000 mV $\rightarrow$ + 1000 mV $\rightarrow$ - 1000 mV. Similar plot, with applied potential (versus reference electrode potential) as a

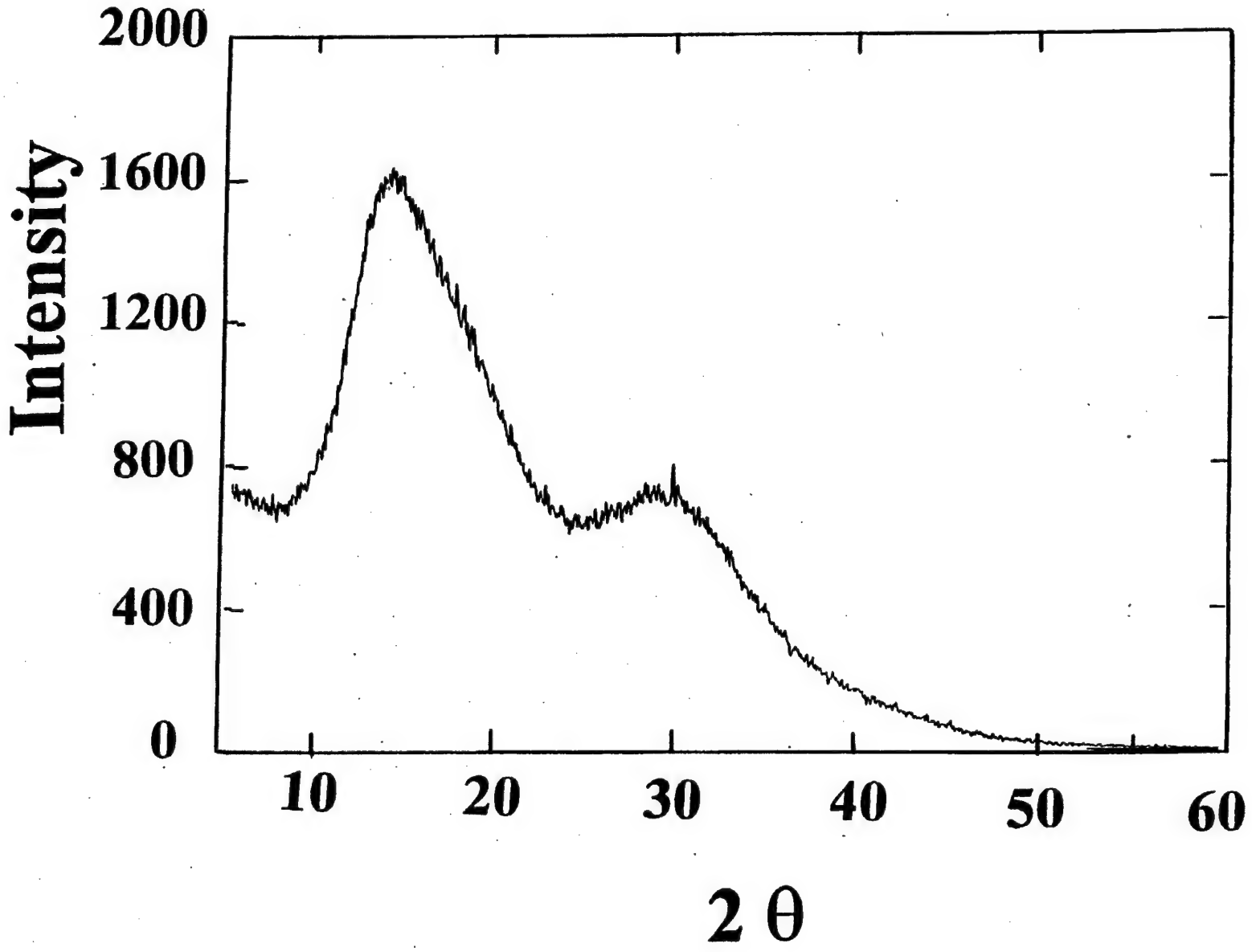

Figure 4. X-ray diffraction pattern or the electrochemical test cell material.

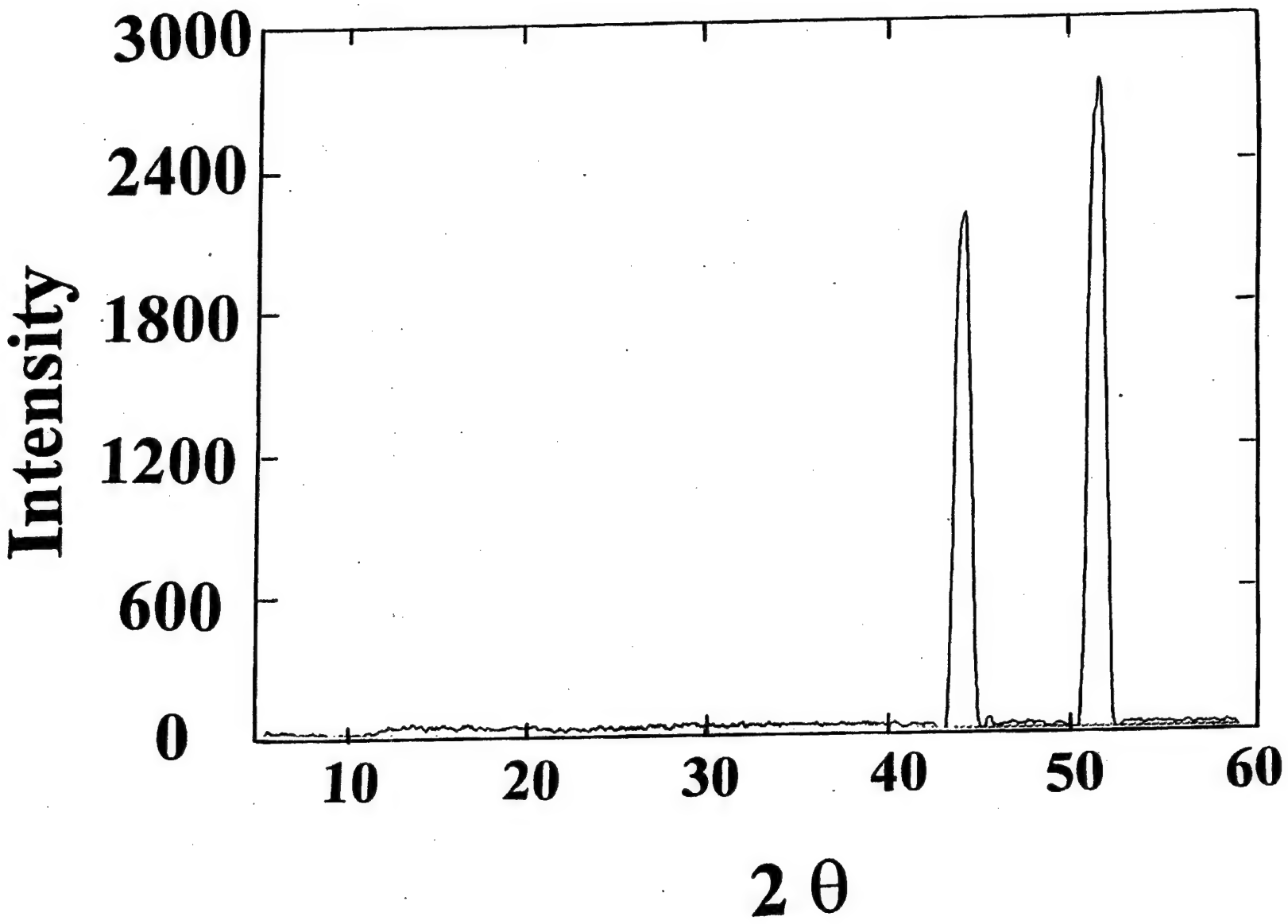

Figure 5. X-ray diffraction of nickel foil after subtracting the contribution due to the cell material.

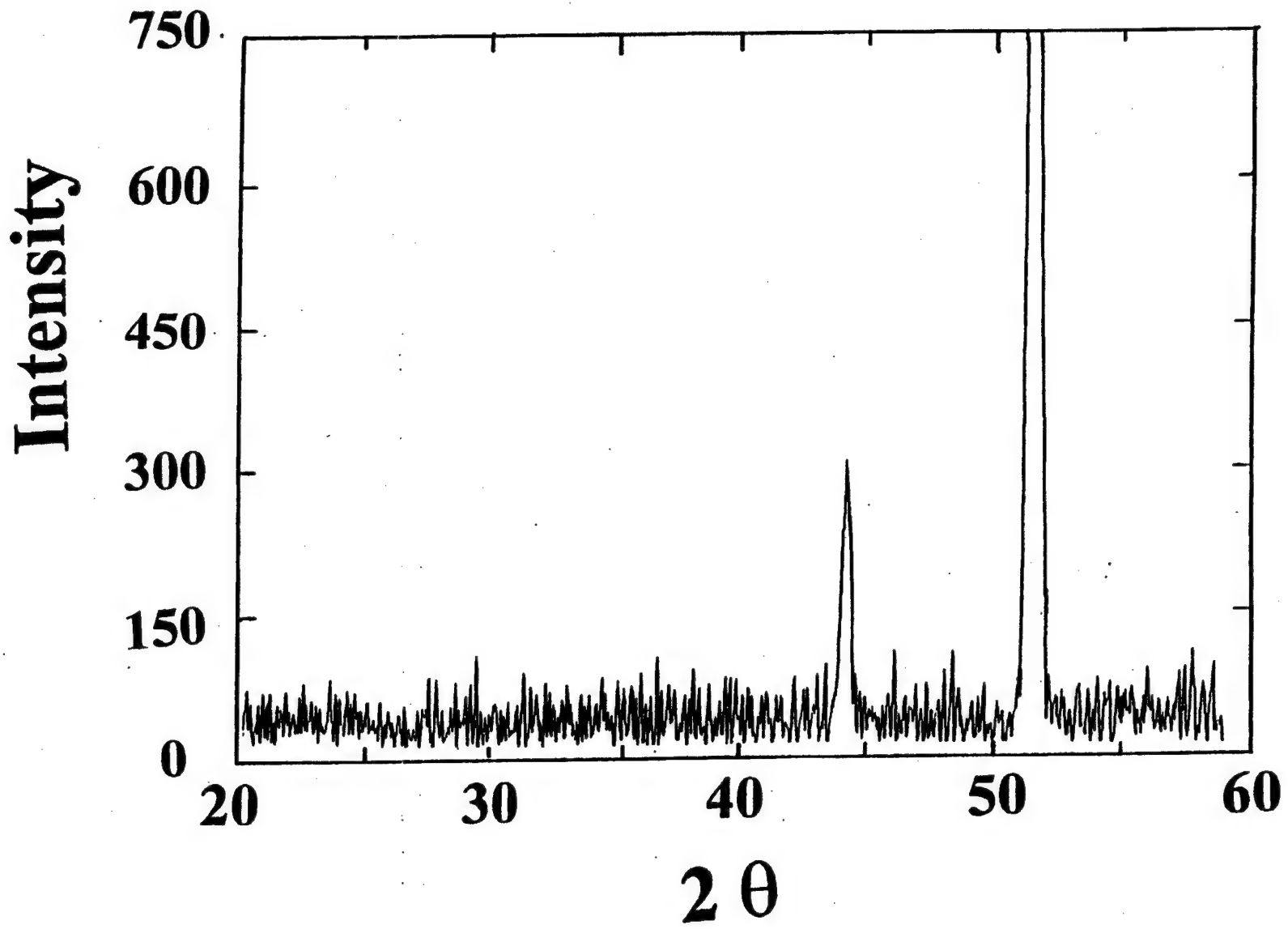

Figure 6. Typical x-ray diffraction pattern obtained from 12.5μm (0.0005") thick nickel foil mounted on the electrochemical test cell.

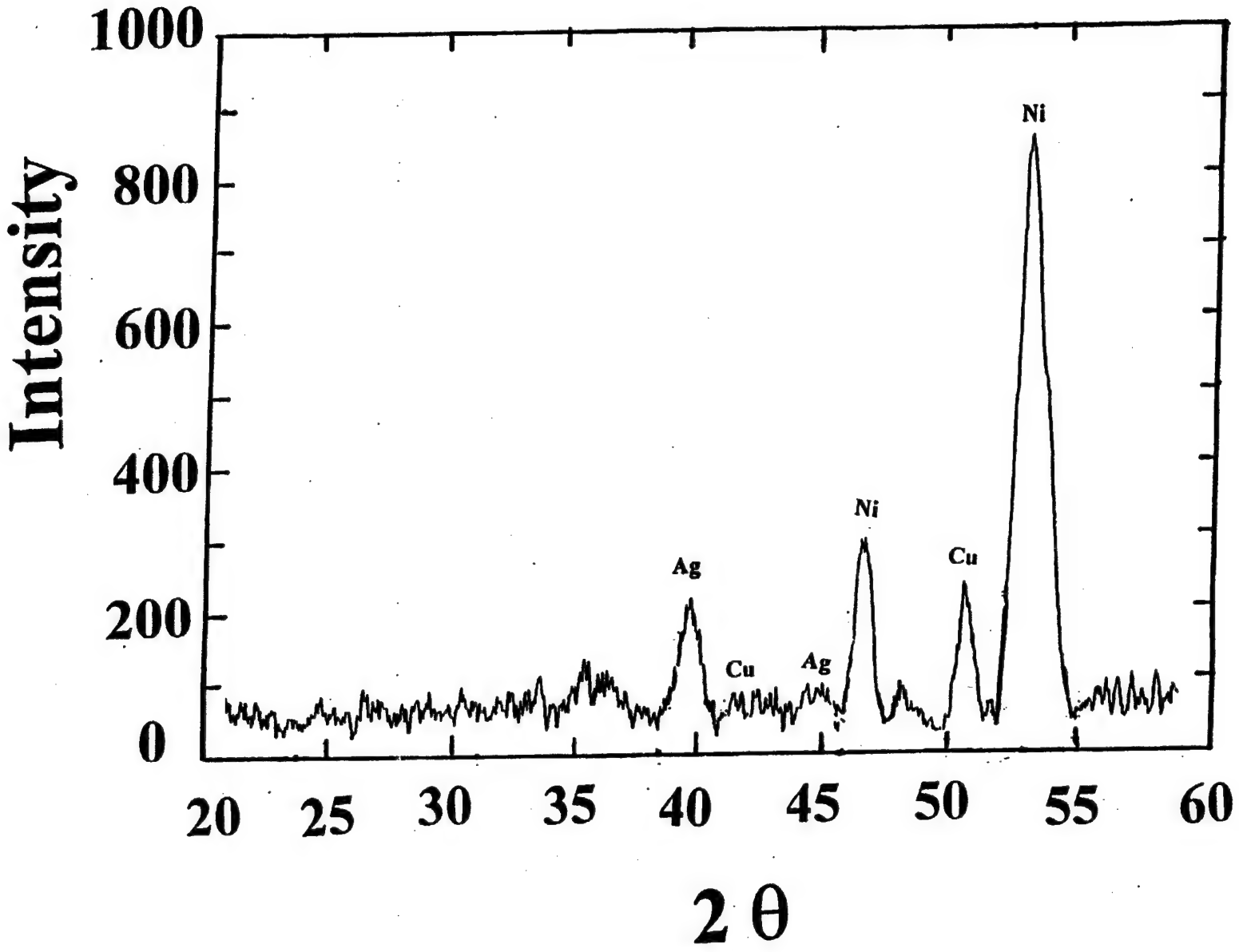

Figure 7. X-ray diffraction pattern of thin nickel foil and silver foil composite laminated on a copper back plate.

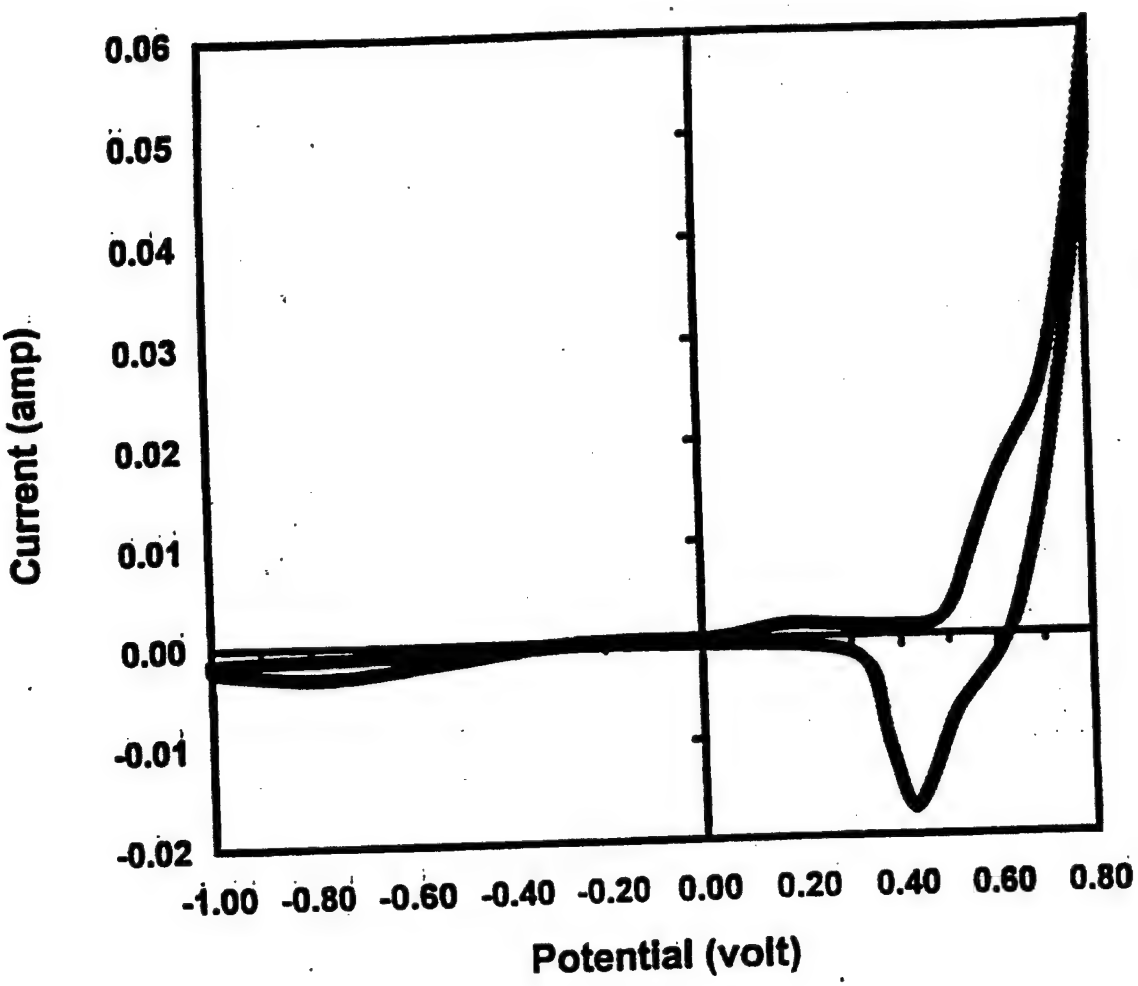

Figure 8. Potential versus current plot of nickel in sea water solution at room temperature.

function of log current density is shown in Figure 9. From Figures 8 and 9 it can be suggested that the sections of different oxidation states can be better represented on the log current density versus applied potential plot. The results (shown in Figure 8) also suggest that as the polarity of the applied potential changes a major change starts to take place around + 100 mV with a maximum conversion at and around + 450 mV.

The test cell was filled with the sea water solution that was pre-electrolyzed in order to remove any cationic impurities. Due care was taken during the filling of the test cell to ensure that no air bubbles were trapped between the nickel foil and the solution. The test cell was attached to the x-ray unit and the x – ray diffraction spectrum of the nickel foil and the nickel / sea water interface was obtained. Later the electrochemical testing was initiated. Two pre-selected constant potentials (- 800 mV and + 450 mV) were applied continuously during each electrochemical study period of nearly 72 hours.

XRD RESULTS FOR POTENTIALS OF – 800 mV

Figure 10 shows a typical x-ray diffraction pattern obtained for the nickel / sea water interface, without the application of any electrical potential. The results indicate that some oxidation has occurred and the surface layers of nickel were converted to γ - NiOOH.

When a cathodic potential of - 800 mV was applied to the nickel foil in sea water solution, during the first 60 minutes, no significant changes were observed in the diffraction pattern. However, a careful examination of x-ray scans acquired later revealed that the possible changes were masked by the system's background noise. After one hour, significantly measurable differences in the diffraction patterns were observed. Figures 11

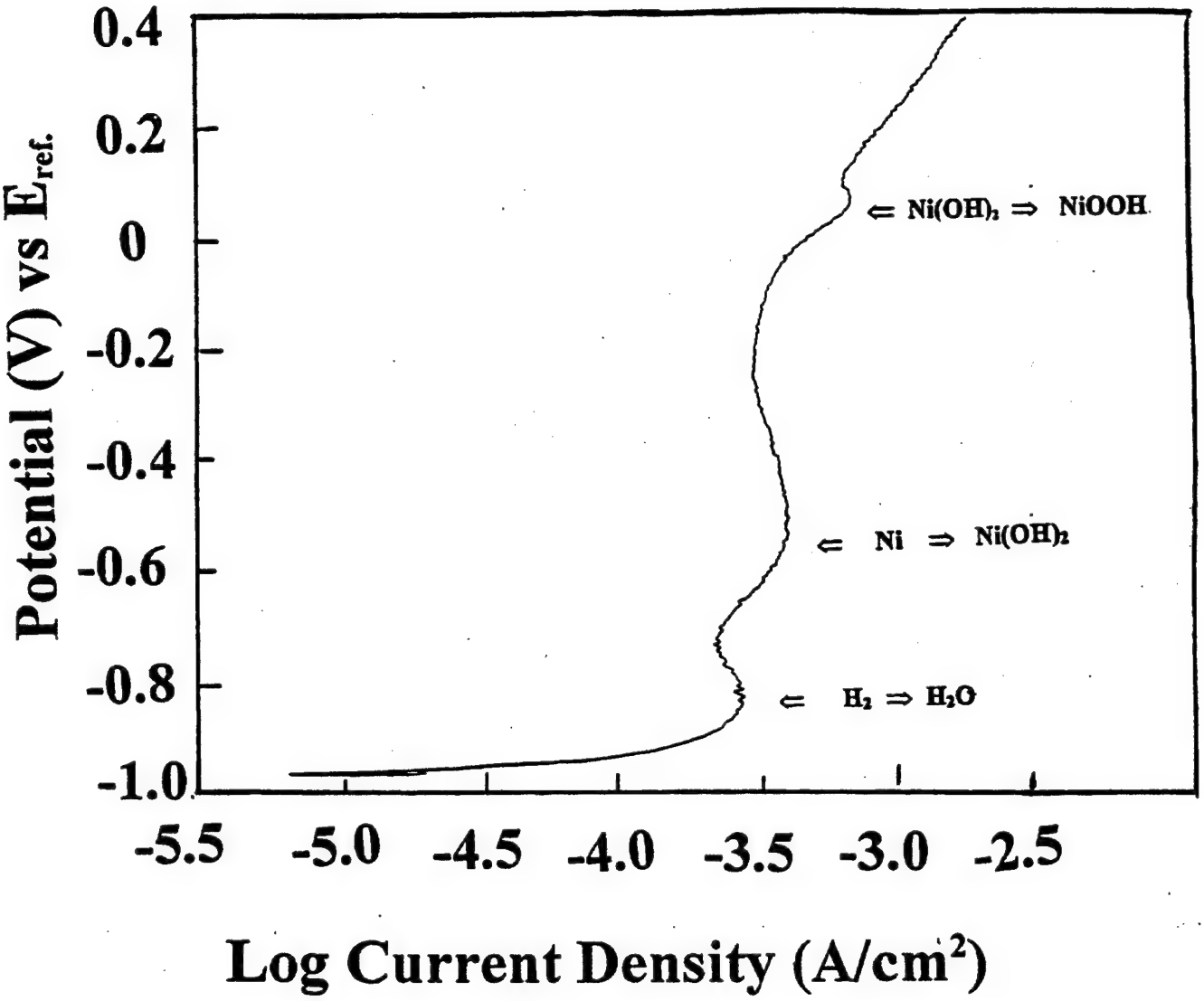

Figure 9. Log current density versus applied potential (versus reference potential) plot of nickel/sea water system at room temperature.

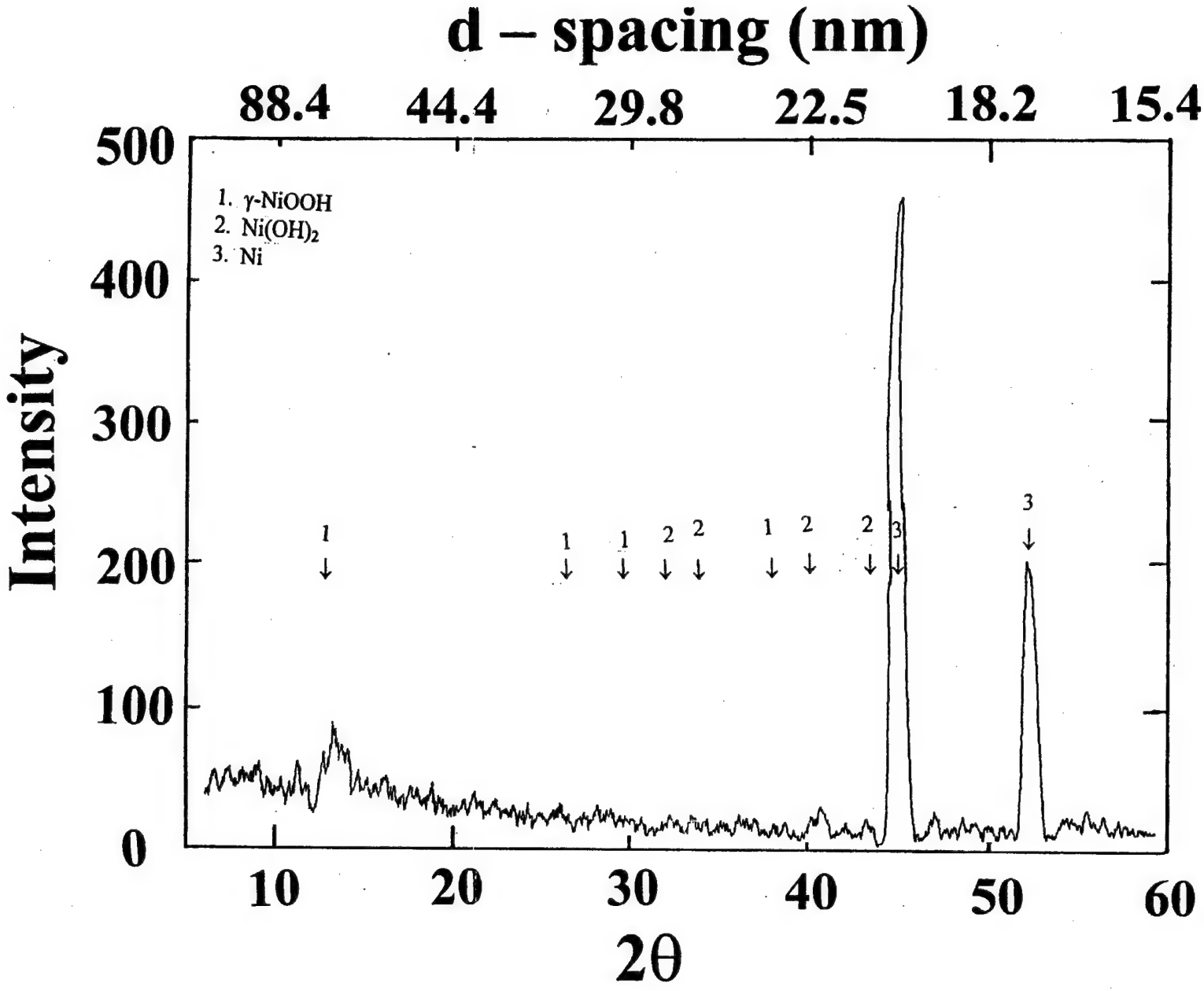

Figure 10. In-situ x-ray diffraction pattern obtained 12.5 μm (0.0005") thick nickel foil mounted on the electrochemical test cell filled with sea water

- 15 show typical x-ray diffraction patterns obtained after 1, 2, 4, 6 and ~ 24 hours of exposure. Between 24 – 48 hours, the x-ray diffraction patterns did not reveal any significant structural changes. Between 48 - 72 hours, the test samples tended to develop fine pores and the electrolyte would seep through the exposed film surface. Unlike nickel / KOH system in which some foils were completely destroyed due to contact with the KOH solution over long periods of time, no foils were completely destroyed by the sea water solution. The results shown in Figures 11 – 15 suggest that the concentration of γ - NiOOH increases initially with an increase in the electrochemical processing time. After 4 hours, at – 800 mV the $Ni(OH)_2$ phase tends to grow at the expense of γ - NiOOH.

When a constant - 800 mV was continuously applied, the cathodic reaction progresses with the accumulation of OH at the cathode and the progression of the reaction from nickel interface can be represented as:

$$\gamma \text{ - NiOOH} \Rightarrow Ni(OH)_2 \Rightarrow H2 \uparrow$$

$$H_2O \Rightarrow OH^- + \tfrac{1}{2} H_2\uparrow$$

$$Ni^{3+}OOH \Rightarrow Ni^{2+}(OH)_2 \Rightarrow H_2O \Rightarrow \tfrac{1}{2} H2 \text{ gas} \uparrow + (OH)^-$$

XPS RESULTS FOR POTENTIALS OF – 800 mV

After the in-situ examination of the nickel sample in sea water for 24 hours was completed, the nickel foil was removed from the test cell and was rinsed with distilled water. The sample was then introduced into the sample chamber of the XPS unit and was analyzed. The total duration of sample removal from test cell, cleaning, introduction in the XPS unit, and data collection was approximately 20 minutes. Figures 16 and 17 show

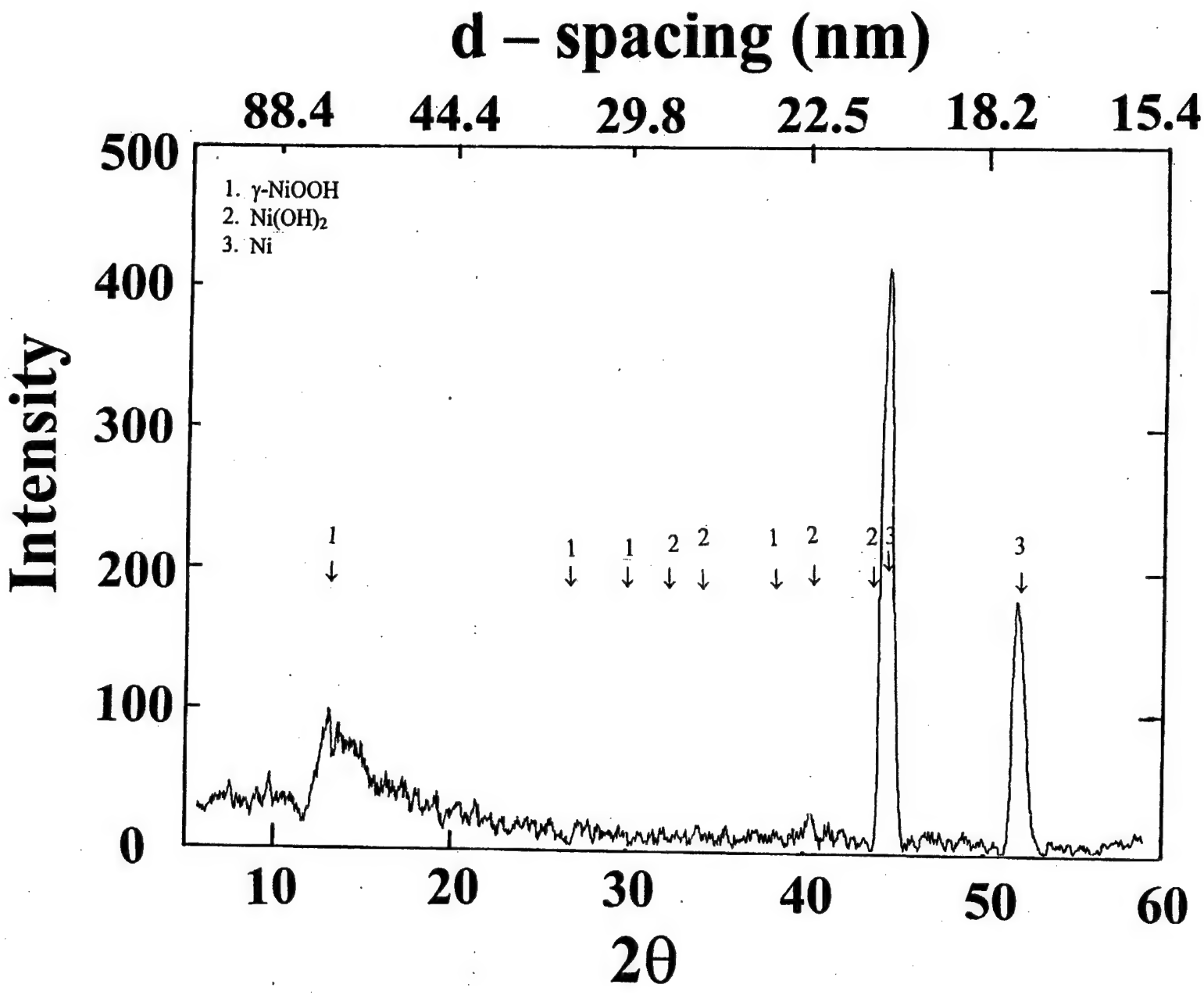

Figure 11. In-situ x-ray diffraction pattern obtained 12.5 μm (0.0005") thick nickel foil mounted on the electrochemical test cell, at - 800 mV versus Ni/NiO after 1 hour.

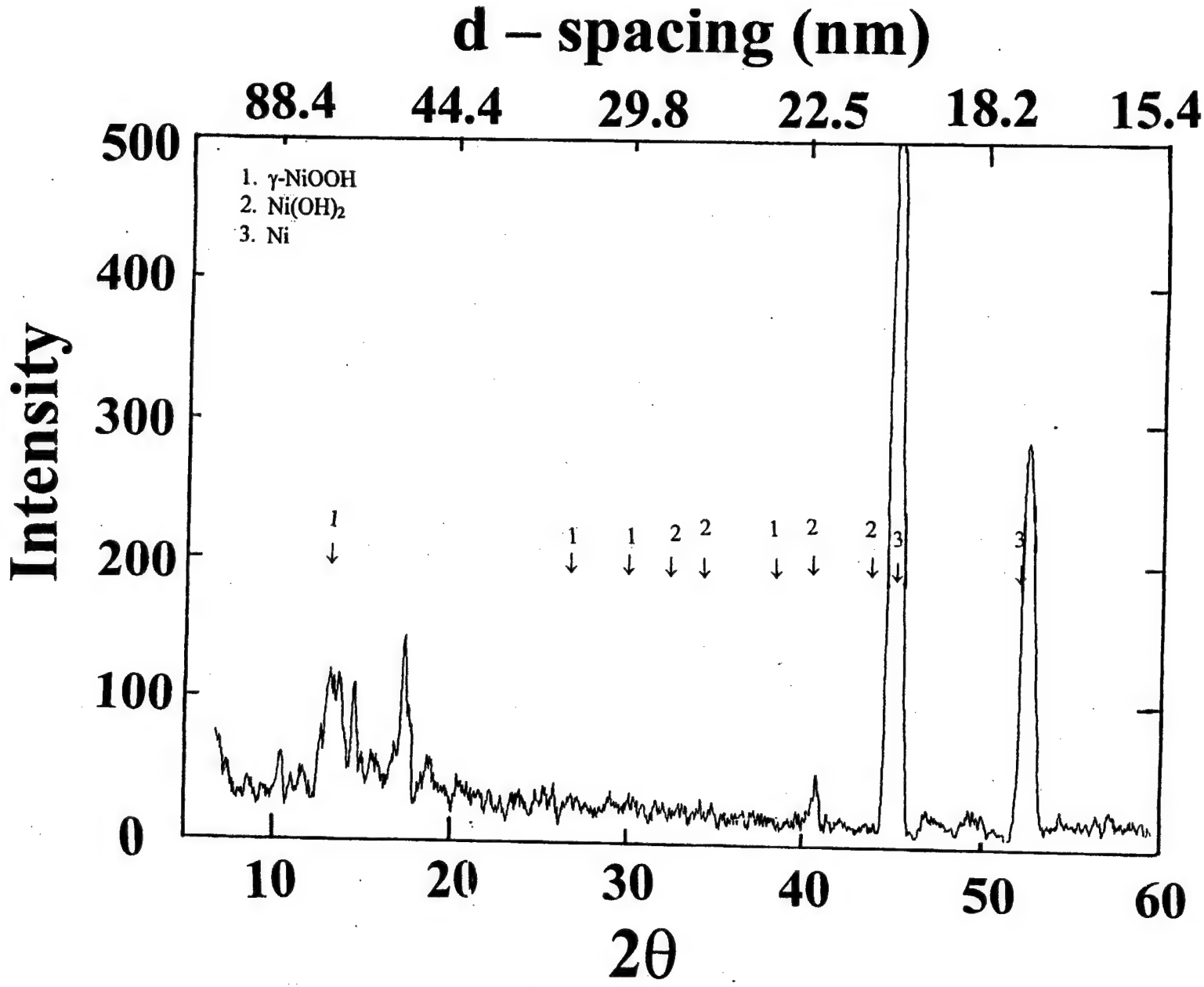

Figure 12. In-situ x-ray diffraction pattern obtained 12.5 μm (0.0005") thick nickel foil mounted on the electrochemical test cell at - 800 mV versus Ni/NiO after 2.0 hours.

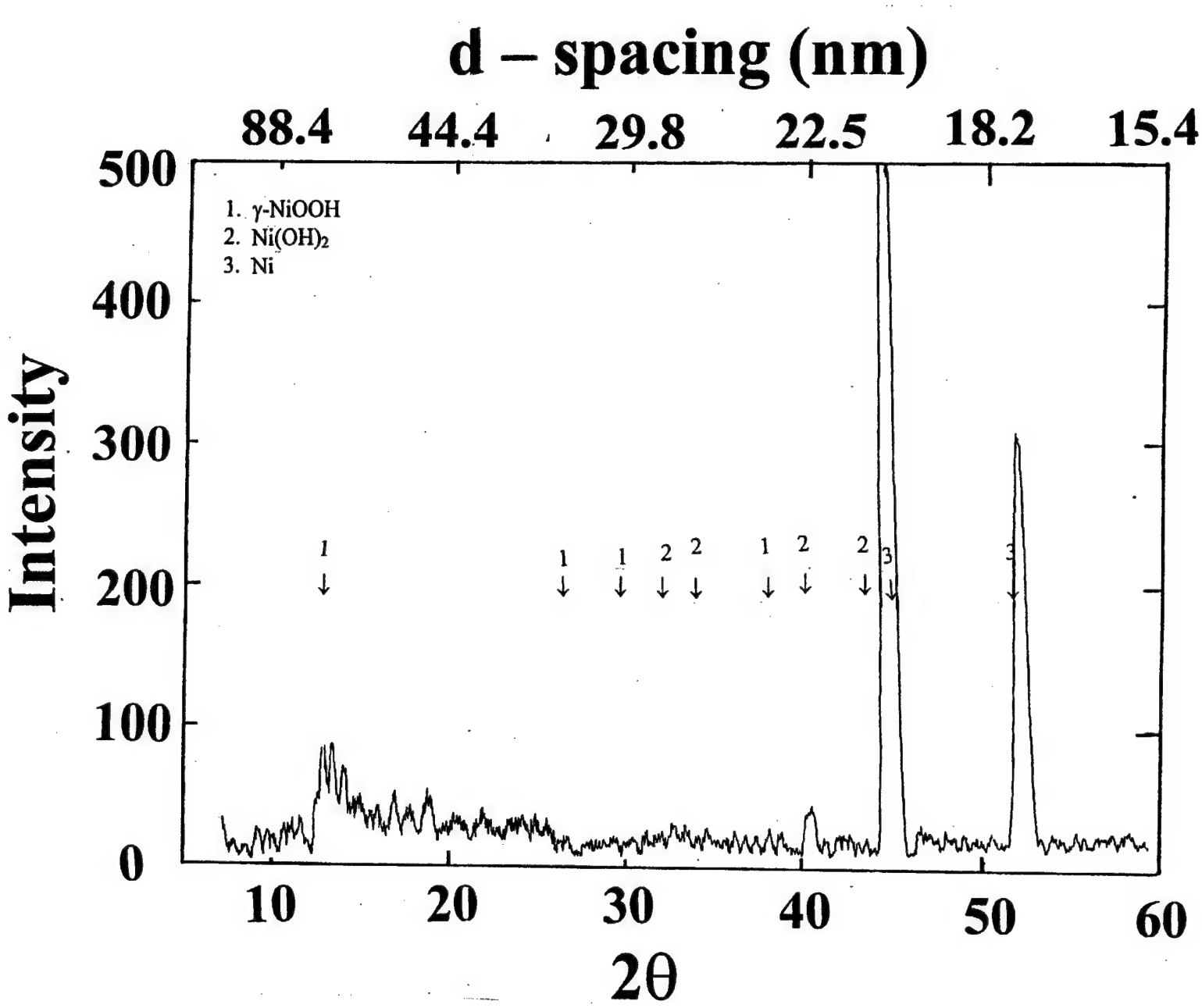

Figure 13. In-situ x-ray diffraction pattern obtained 12.5 μm (0.0005") thick nickel foil mounted on the electrochemical test cell, at - 800 mV versus Ni/NiO after 4 hours.

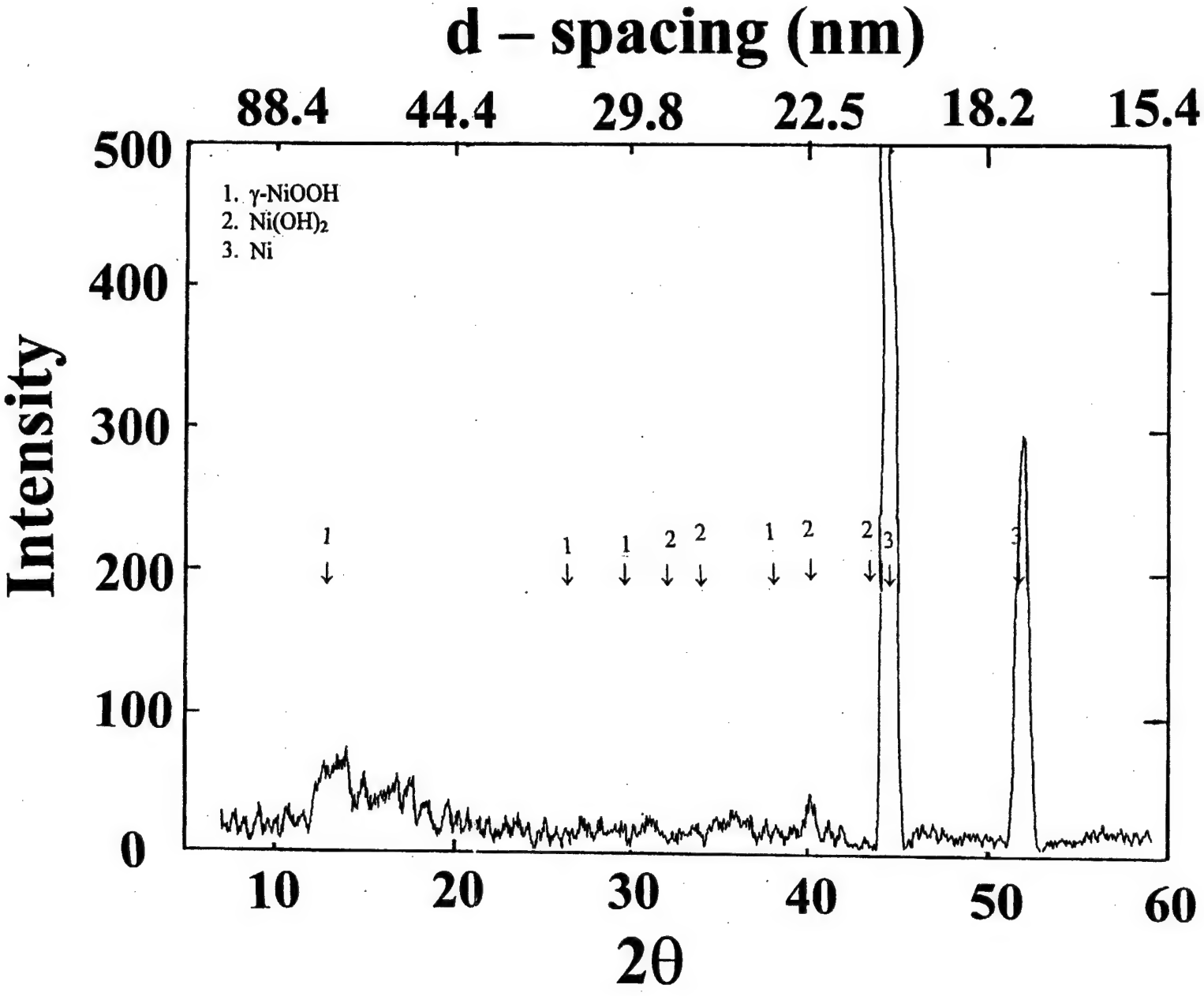

Figure 14. In-situ x-ray diffraction pattern obtained 12.5 μm (0.0005") thick nickel foil mounted on the electrochemical test cell, at - 800 mV versus Ni/NiO after 6.0 hours.

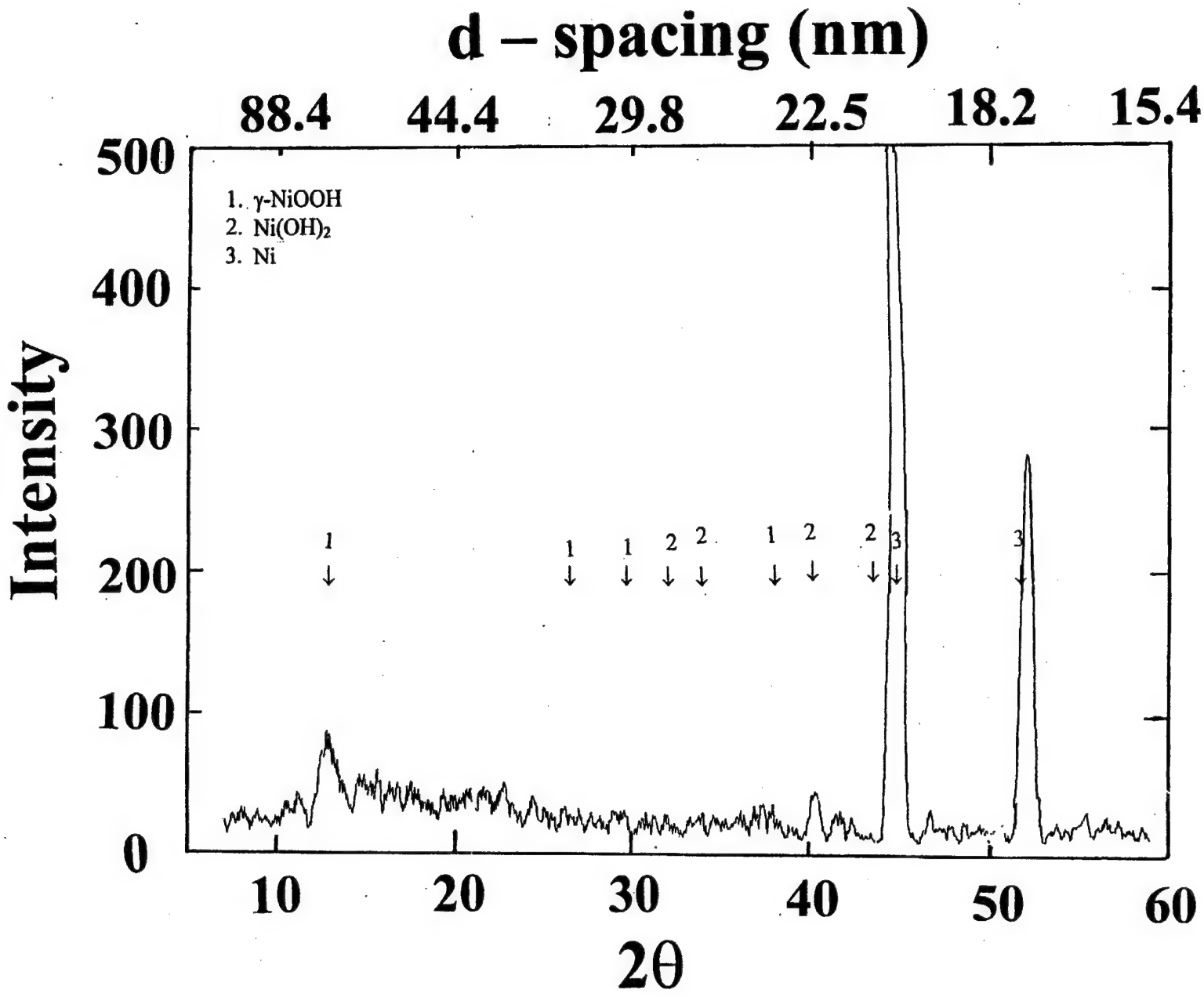

Figure 15. In-situ x-ray diffraction pattern obtained 12.5 μm (0.0005") thick nickel foil mounted on the electrochemical *test* cell, at - 800 mV versus Ni/NiO after 24.0 hours.

typical XPS spectra for nickel and oxygen obtained from the test foil subjected to - 800 mV in sea water solution. The peak locations for various identified compounds were obtained from reference XPS standards [16].

The results in Figure 16 suggest that only $Ni(OH)_2$ is present in the outer passive layer. The detected structure in Figure 17 of oxygen at 532 eV corresponds to the oxygen associated with water of hydration.

XRD RESULTS FOR POTENTIALS OF + 450 mV

Figure 18 shows the x-ray diffraction pattern obtained from 12.5 μm (0.0005") thick nickel foil that is in contact with sea water. Figures 19 – 23 shows the structure of the above foil subjected to a potential of + 450 mV. The figures correspond to the measurements made at time intervals 1, 2, 4, 6 and 24 hours exposure respectively. The results suggest that the surface is oxidized with nickel oxidation states of both Ni^{+3} and Ni^{+2}. In addition, the results also show that the surface of the nickel foil contains $Ni(OH)_2$. At + 450 mV, the reaction of nickel in sea water can be postulated as follows:

$$Ni \Rightarrow Ni(OH)_2 \Rightarrow Ni(OH)_2 .0.75\ H_2O \Rightarrow 3Ni(OH)_2 .2\ H_2O$$

$$\Rightarrow Ni^{+3}OOH \Rightarrow Ni^{+3}{}_2O_3 \Rightarrow Ni^{+2}O$$

XPS RESULTS FOR POTENTIALS OF + 450 mV

Figures 24 and 25 show XPS spectrum for nickel and oxygen obtained from test foils after corrosion testing at + 450 mV in sea water solution. The results suggest that the nickel foil involved in electrochemical reaction at + 450 mV in sea water for 24 hours is oxidized. The nickel layers close to the surface are chemically transformed into 90 % Ni_2O_3 and 10 % $Ni(OH)_2$.

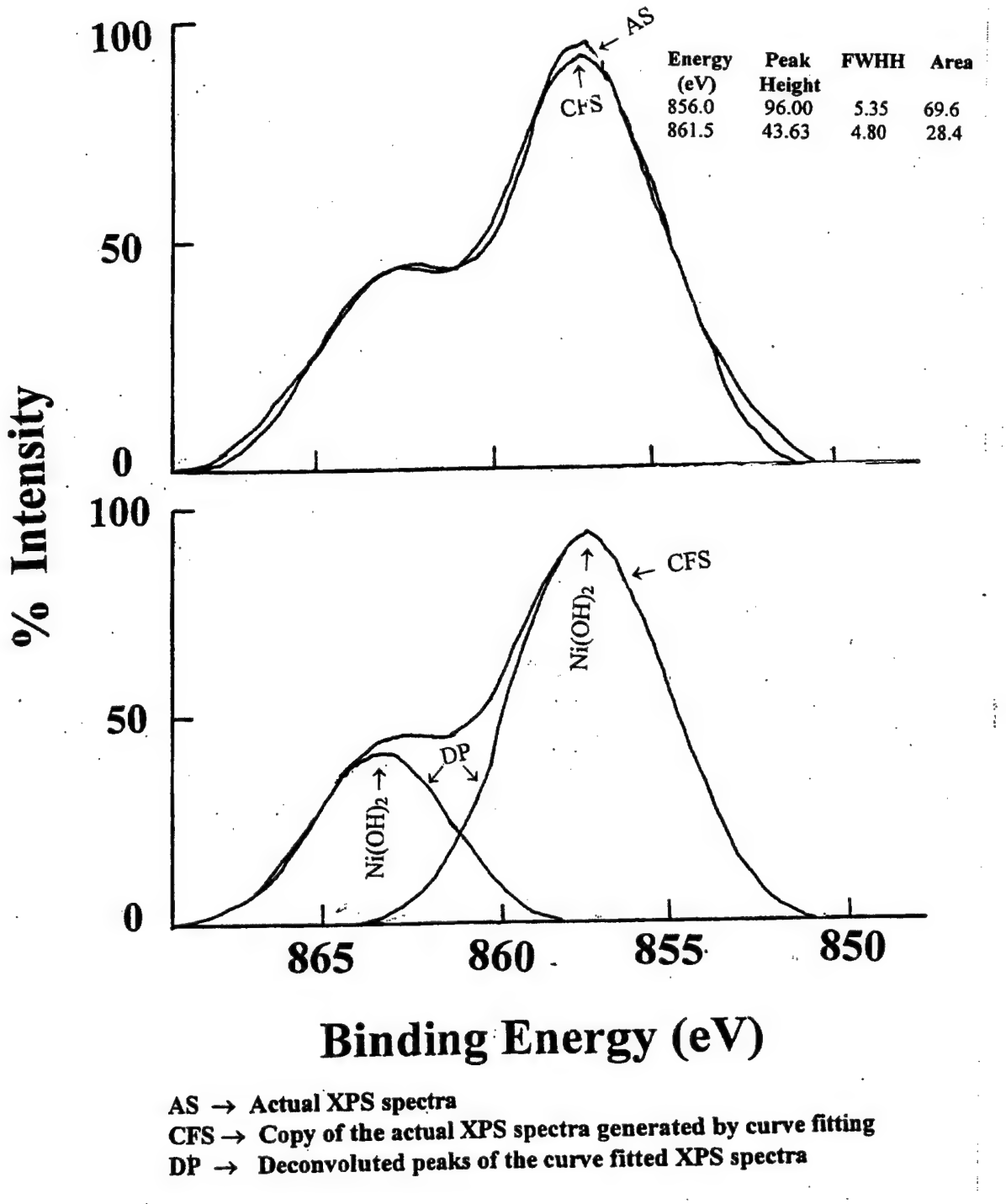

Figure 16. Nickel peaks obtained from XPS analysis of 12.5 μm (0.0005") thick nickel foil surface exposed to sea water at - 800 mV for 24 hours.

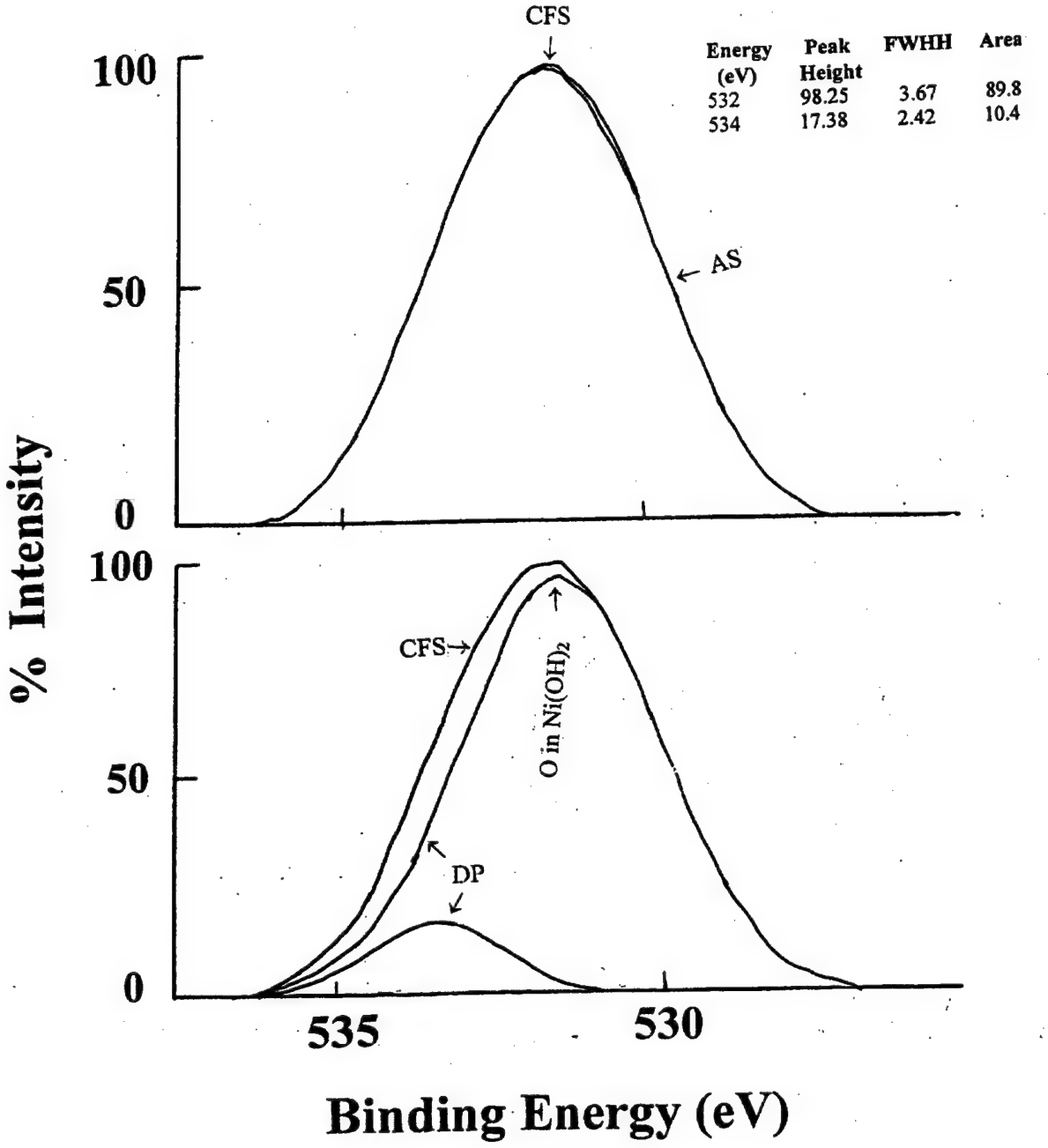

AS → Actual XPS spectra
CFS → Copy of the actual XPS spectra generated by curve fitting
DP → Deconvoluted peaks of the curve fitted XPS spectra

Figure 17. Oxygen peaks obtained from XPS analysis of 12.5 μm (0.0005") thick nickel foil surface exposed to sea water at - 800 mV for 24 hours.

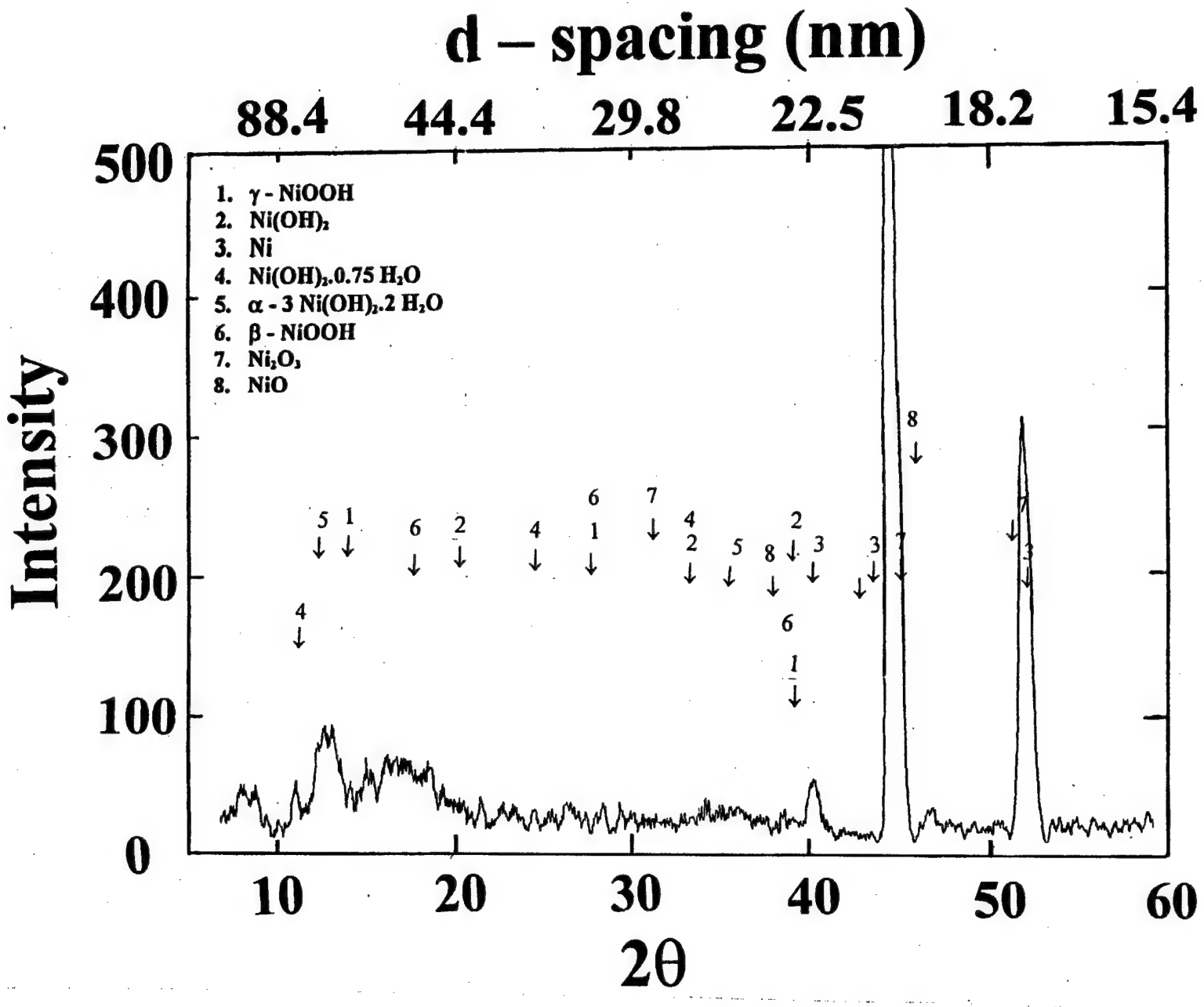

Figure 18. In-situ x-ray diffraction pattern obtained 12.5 μm (0.0005") thick nickel foil mounted on the electrochemical test cell filled with KOH solution.

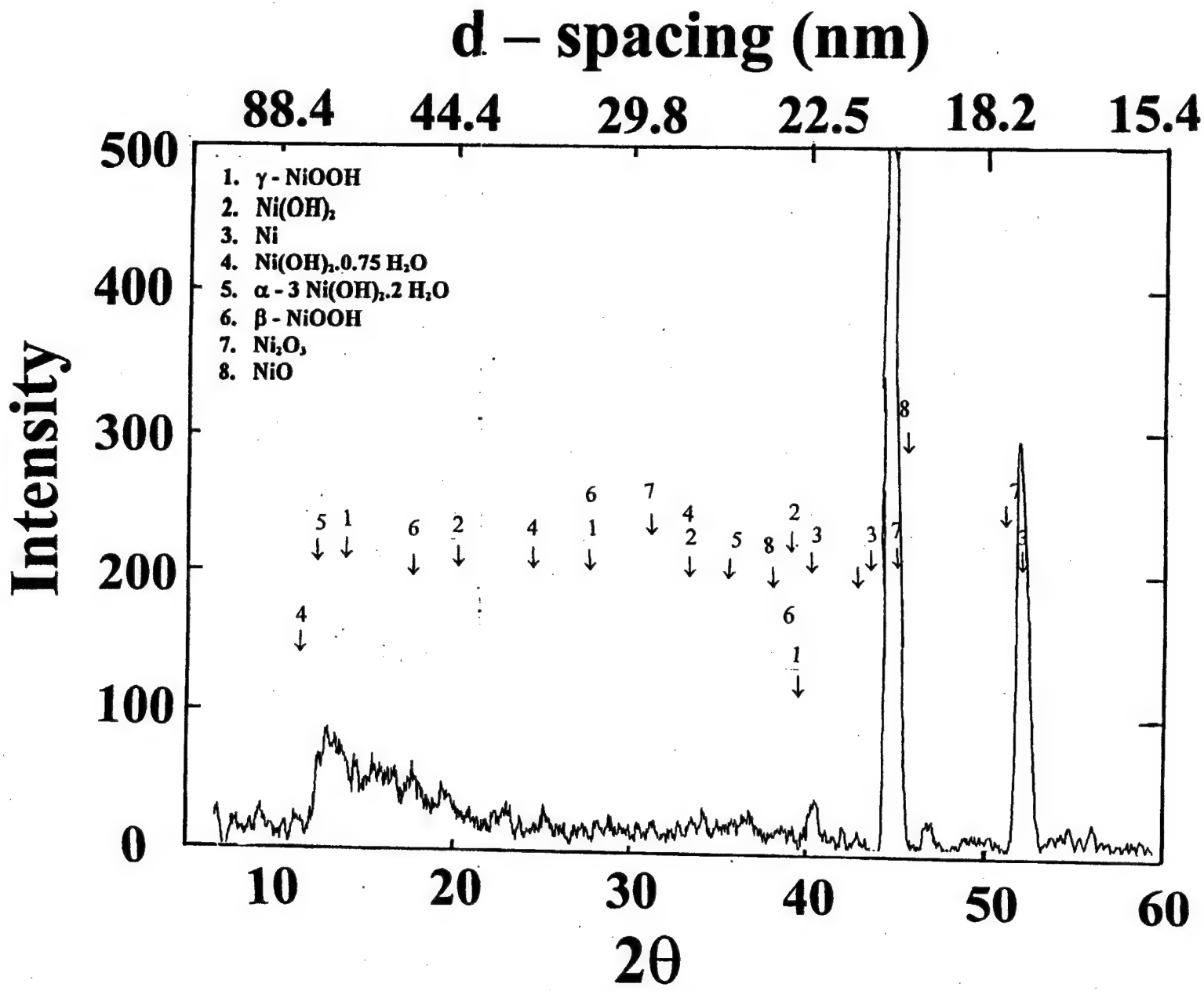

Figure 19. In-situ x-ray diffraction pattern obtained 12.5 μm (0.0005") thick nickel foil mounted on the electrochemical test cell, at + 450 mV versus Ni/NiO after 1.0 hour.

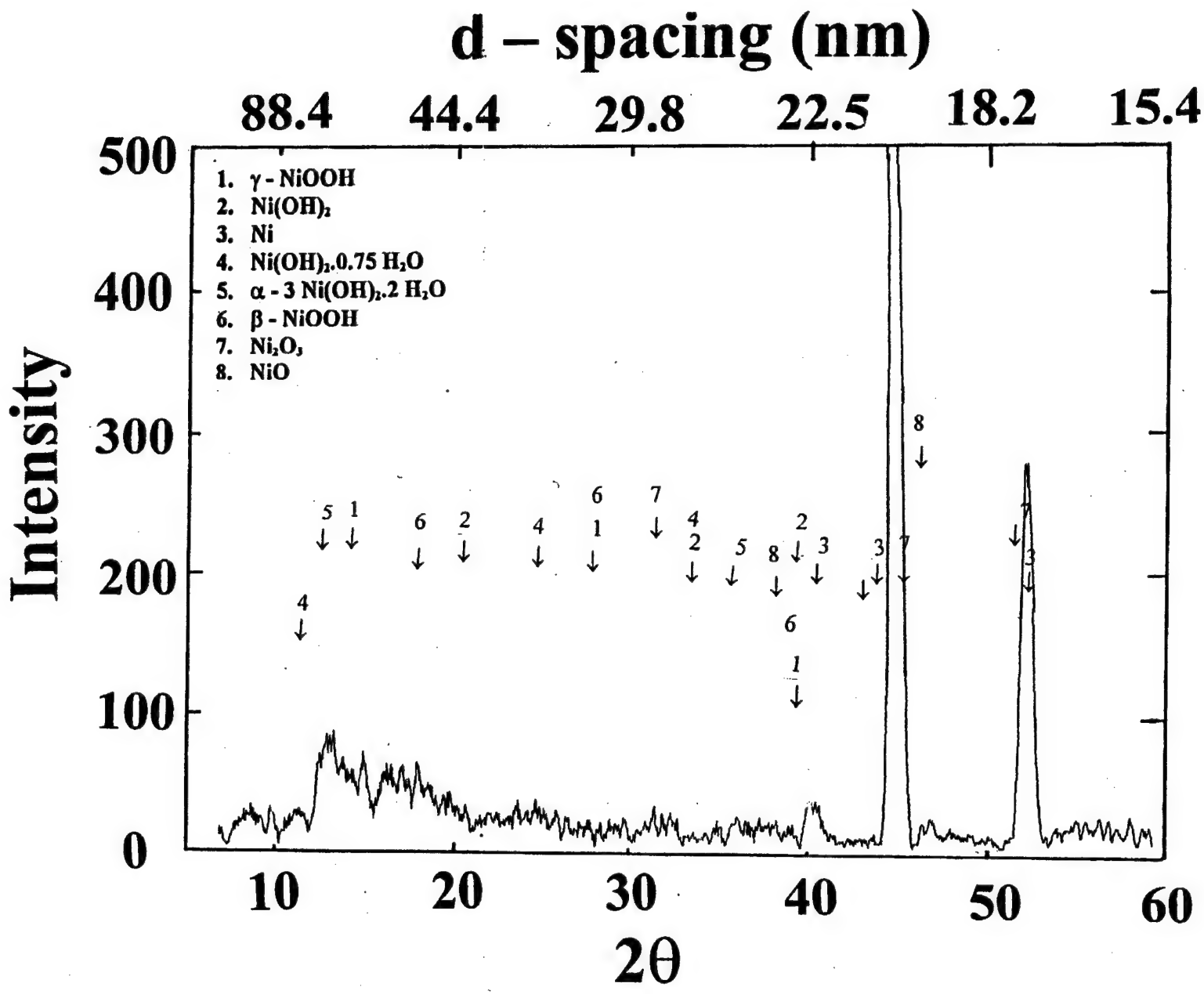

Figure 20. In-situ x-ray diffraction pattern obtained 12.5 μm (0.0005") thick nickel foil mounted on the electrochemical test cell, at + 450 mV versus Ni/NiO after 2.0 hours.

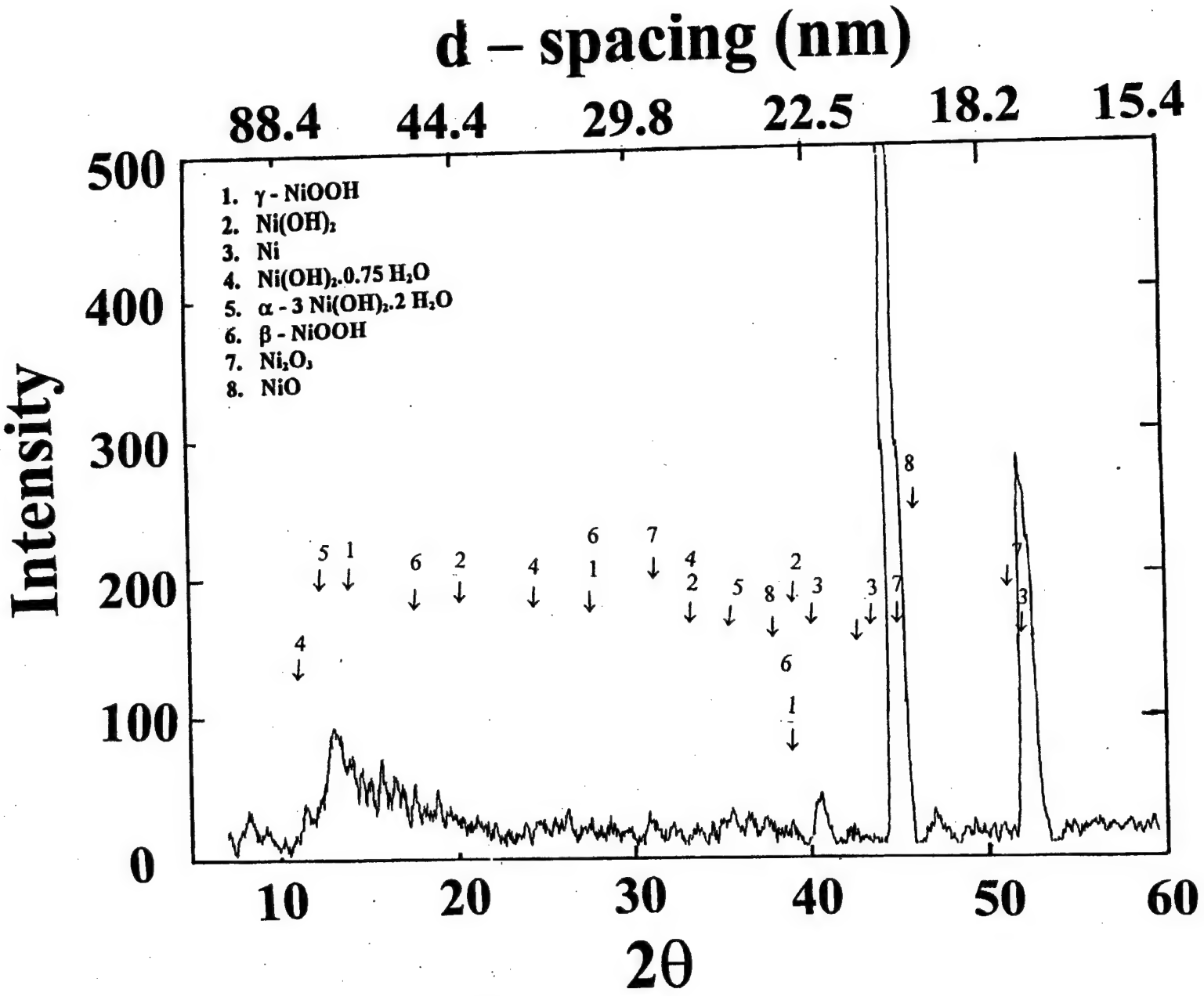

Figure 21. In-situ x-ray diffraction pattern obtained 12.5 µm (0.0005") thick nickel foil mounted on the electrochemical test cell, at + 450 mV versus Ni/NiO after 4.0 hours.

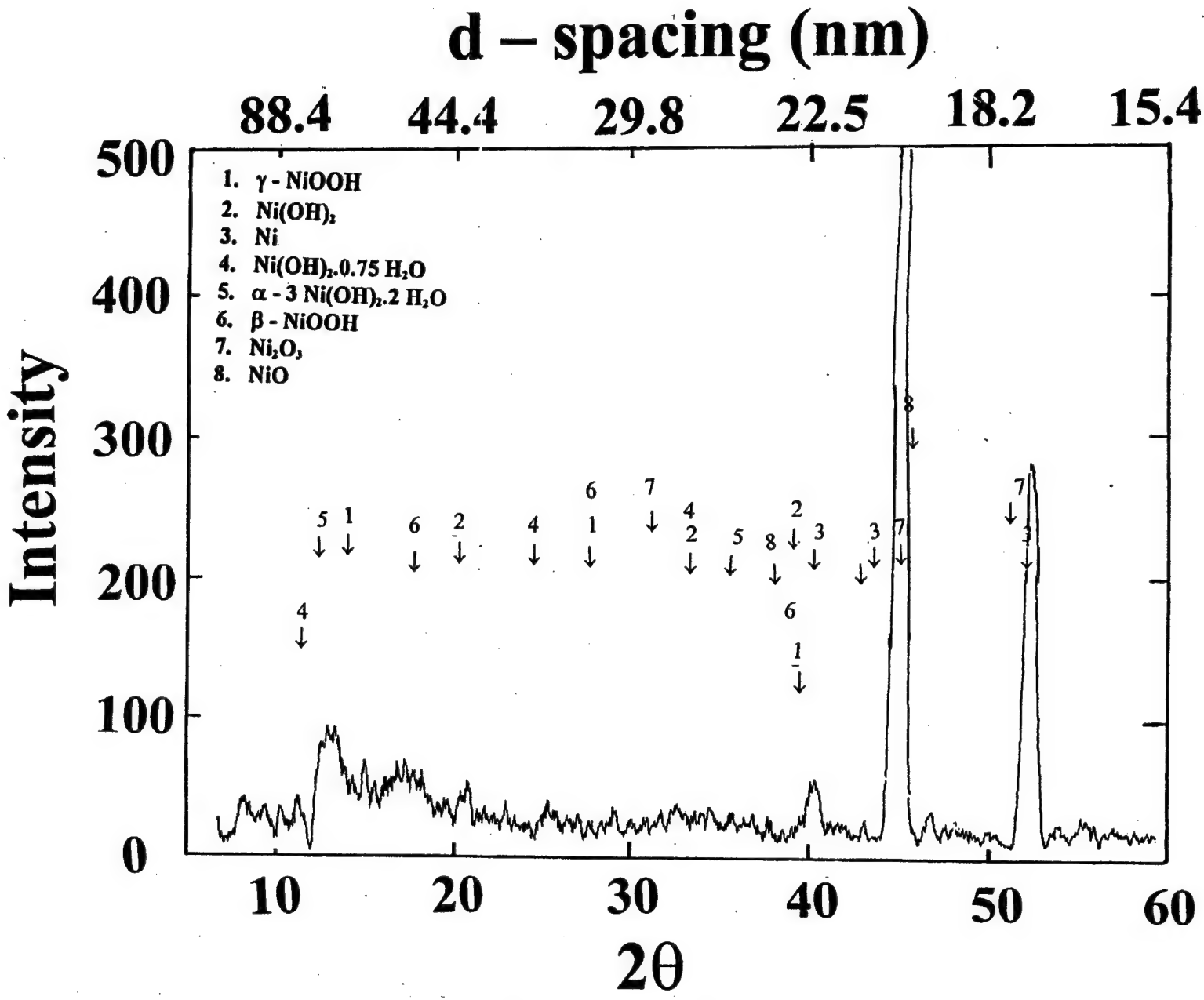

Figure 22. In-situ x-ray diffraction pattern obtained 12.5 μm (0.0005") thick nickel foil mounted on the electrochemical test cell, at + 450 mV versus Ni/NiO after 6.0 hours.

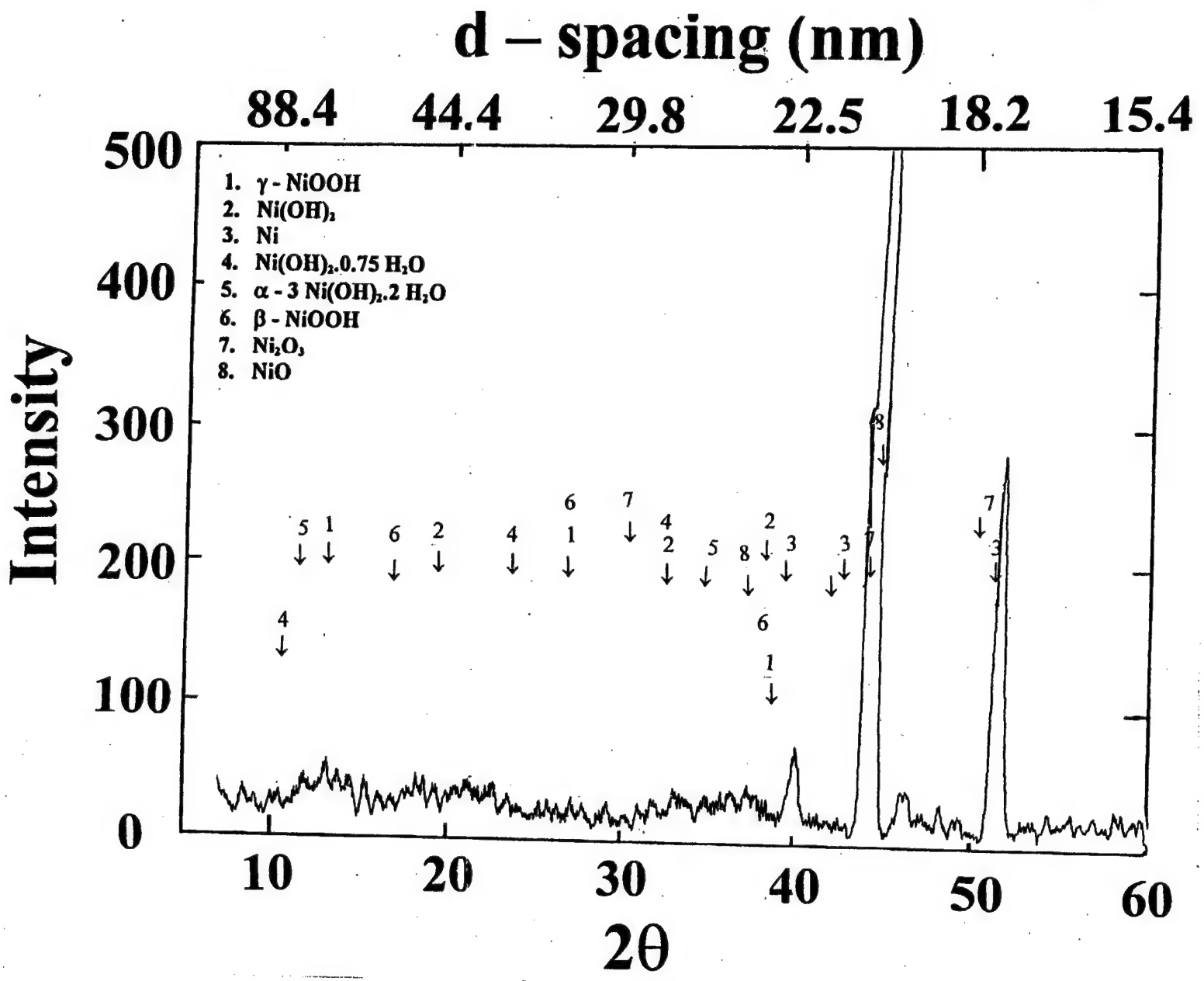

Figure 23. In-situ x-ray diffraction pattern obtained 12.5 μm (0.0005") thick nickel foil mounted on the electrochemical test cell, at + 450 mV versus Ni/NiO after 24.0 hours.

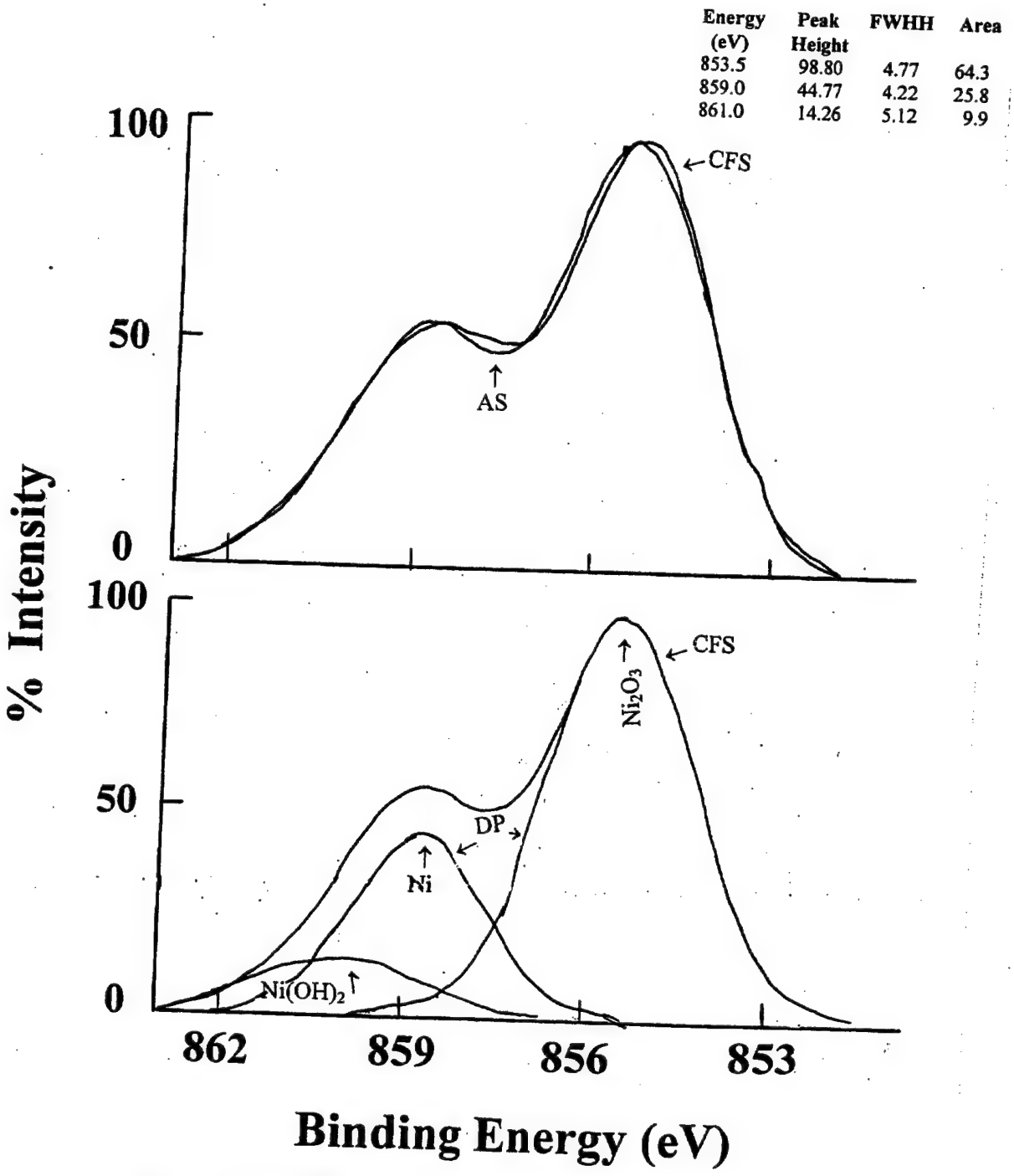

Figure 24. Nickel peaks obtained from XPS analysis of 12.5 μm (0.0005") thick nickel foil surface exposed to the sea water at + 450 mV for 24 hours.

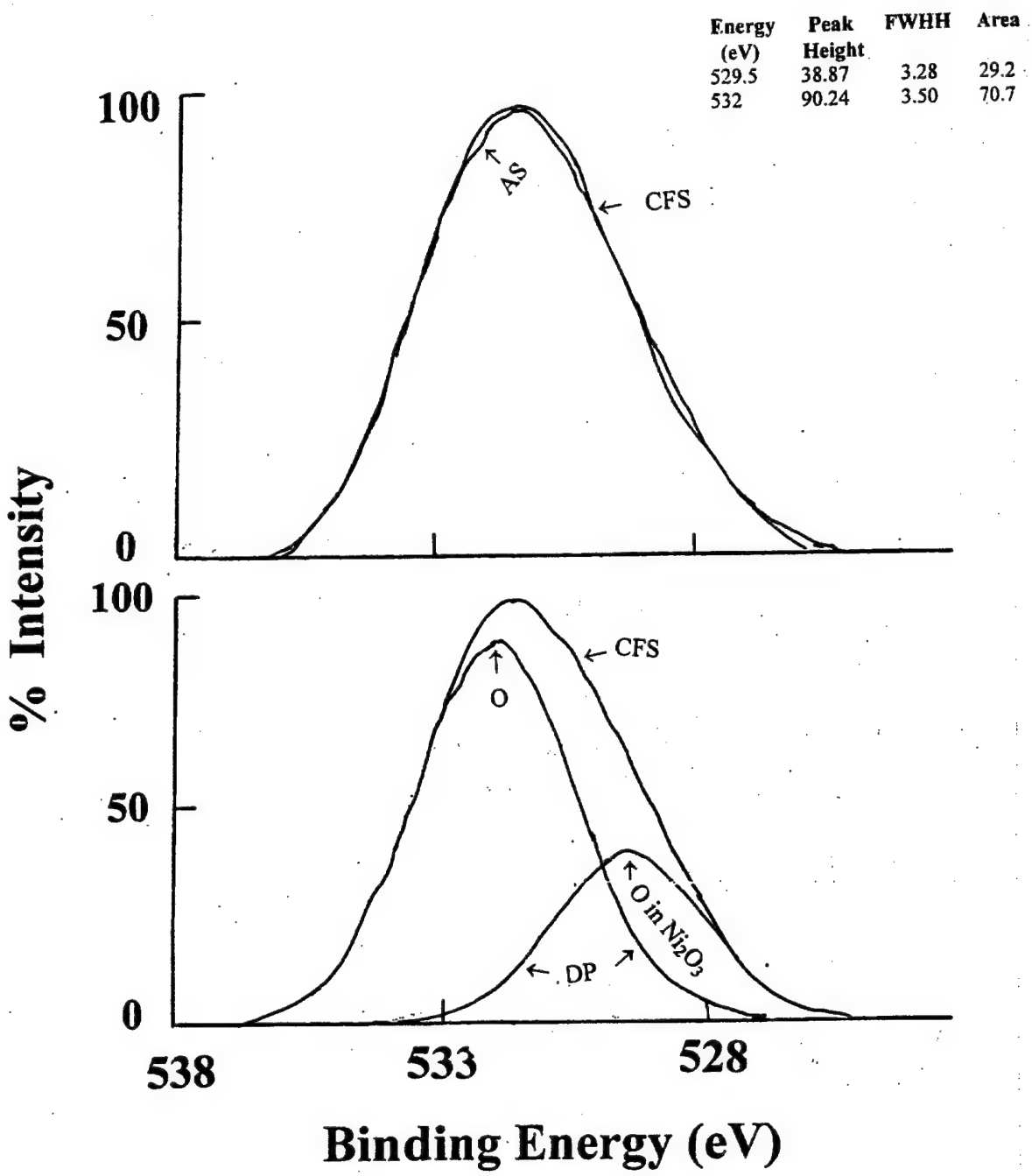

Figure 25. Oxygen peaks obtained from XPS analysis of 12.5 μm (0.0005") thick nickel foil surface exposed to the sea water at + 450 mV for 24 hours.

DISCUSSION

Even though the intensity of the x-ray peaks shown in Figures 11 – 15 and 18 – 23 are not large and the variations could be attributed to the instrumental background noise, in our earlier investigation on nickel / KOH system [10], we found the same two theta values for maximum intensity. The major difference between the nickel / KOH and nickel / sea water systems is the resolution of the intensity maximums. Figures 26 – 34 show typical x-ray diffraction patterns obtained from nickel / KOH system as a function of applied potentials of - 800 mV for 1.5, 2,4 and 24 hours (Figures 26 – 30) and of + 450 mV for 0.5, 1, 3, 4 and 24 hours (Figures 31 – 34) respectively.

By comparing both sets of x – ray diffraction patterns it can be suggested that the weak structural changes observed in nickel / sea water system are real. The unexpected presence of significant amount of γ- NiOOH seen in Ni / KOH system at – 800 mV is not due to the òxidation of Ni to γ - NiOOH, but it is due to the initial chemical reaction between Ni and KOH. From the results it can be postulated that once the γ - NiOOH formed, a few layers of the γ - NiOOH tend to progress inwards into the metal phase. The remaining oxide layers tend to reduce to form $Ni(OH)_2$.

The cathodic reaction progression of the cathodic electrochemical reaction in nickel / sea water at – 800 mV can be represented as:

$$Ni^{+3} \Rightarrow Ni(OH)_2 \Rightarrow H2 \uparrow$$

$$H_2O \Rightarrow OH^- + ½\, H_2\uparrow$$

$$Ni^{3+}OOH \Rightarrow Ni^{2+}(OH)_2 \Rightarrow H_2O \Rightarrow ½\ H2\ gas \uparrow + (OH)^-$$

At + 450 mV, a few layers of the initial γ - NiOOH that was formed due to chemical reaction between nickel and sea water or KOH tend to migrate into the metal

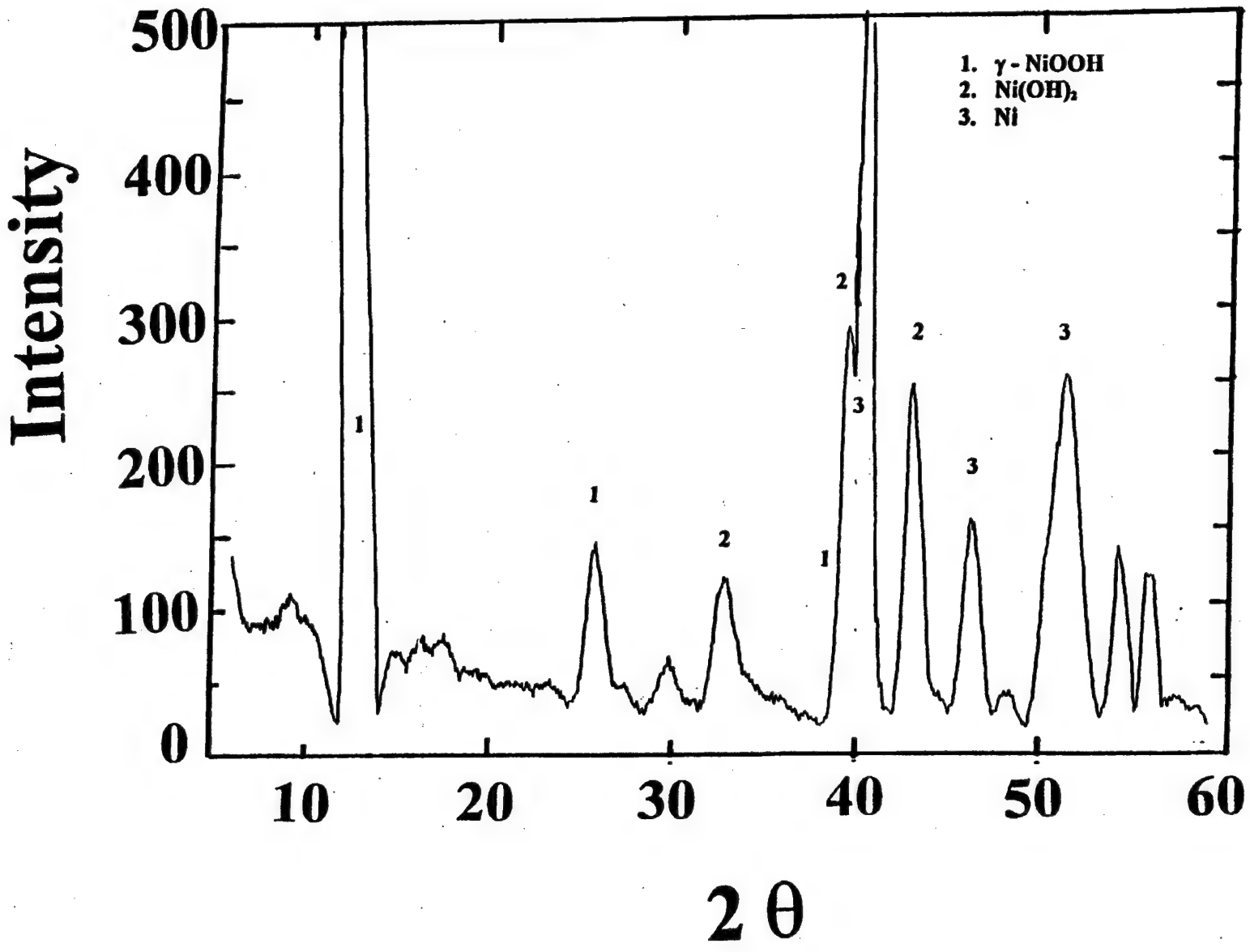

Figure 26. In-situ x-ray diffraction pattern obtained for 12.5 μm (0.0005") thick nickel foil mounted on the electrochemical test cell filled with KOH, after exposure for 1.5 hour at - 800 mV versus a Ni/NiO electrode.

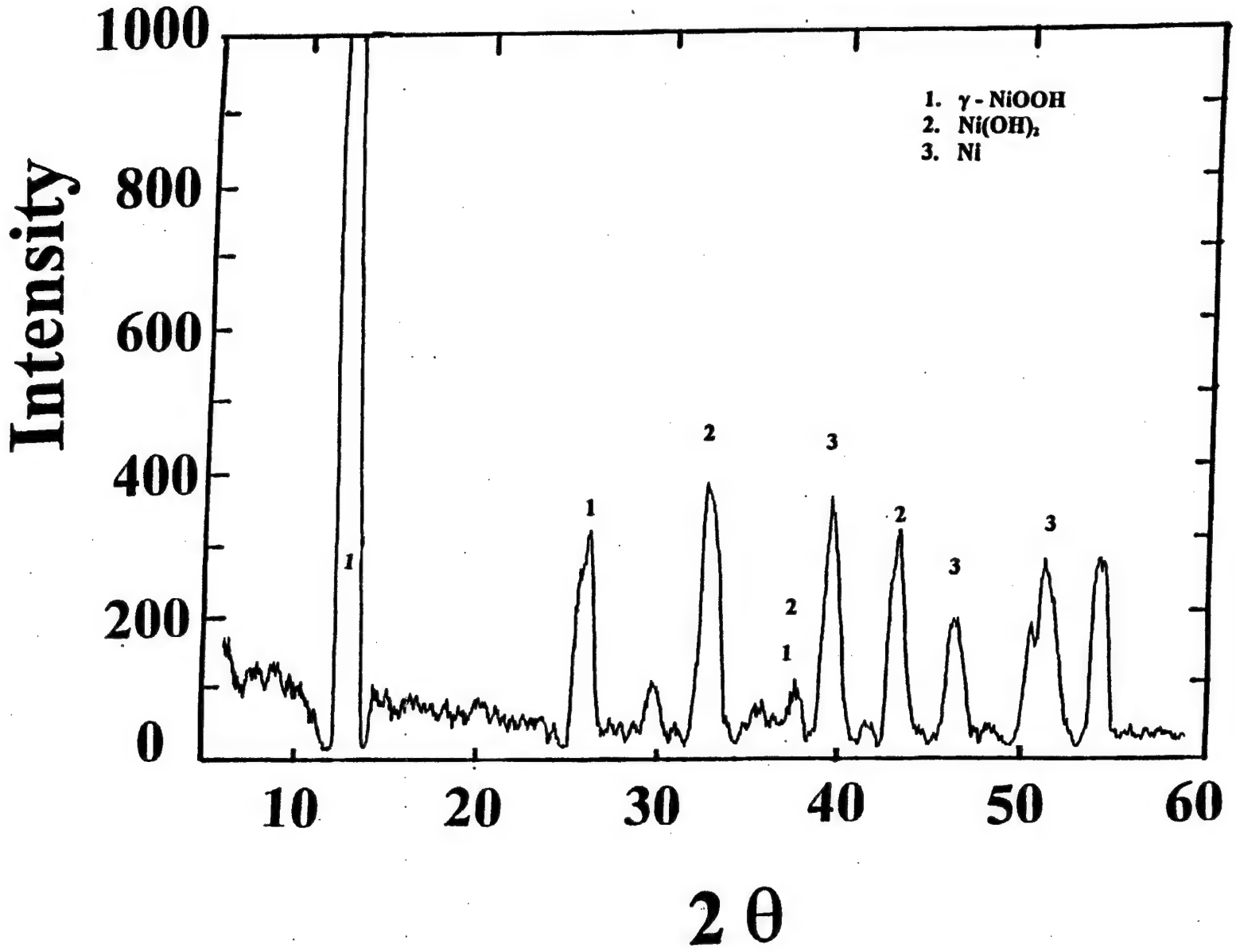

Figure 27. In-situ x-ray diffraction pattern obtained for 12.5 μm (0.0005") thick nickel foil mounted on the electrochemical test cell filled with KOH, after exposure for 2 hours at - 800 mV versus a Ni/NiO electrode.

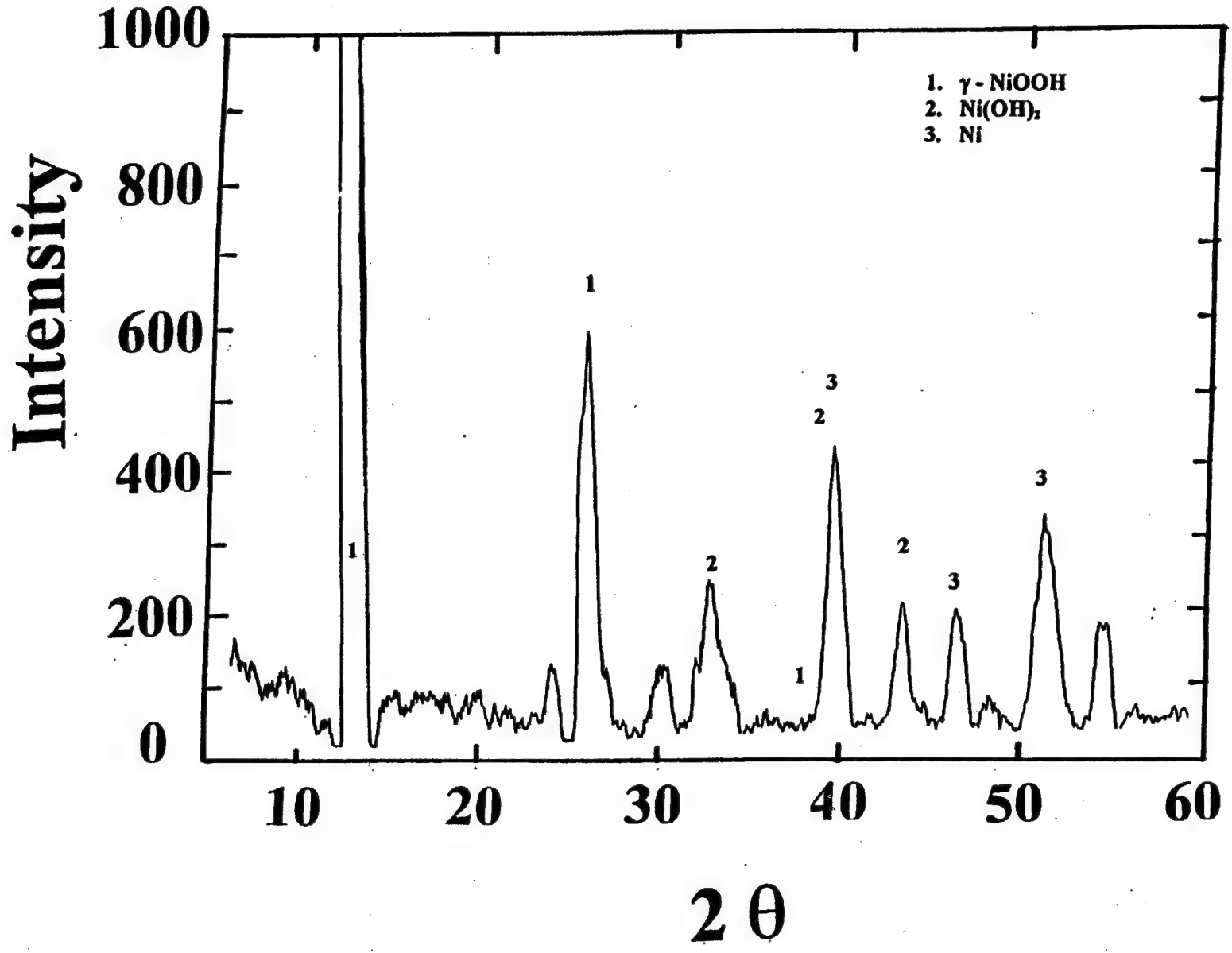

Figure 28. In-situ x-ray diffraction pattern obtained for 12.5 μm (0.0005") thick nickel foil mounted on the electrochemical test cell filled with KOH, after exposure for 3 hours at - 800 mV versus a Ni/NiO electrode.

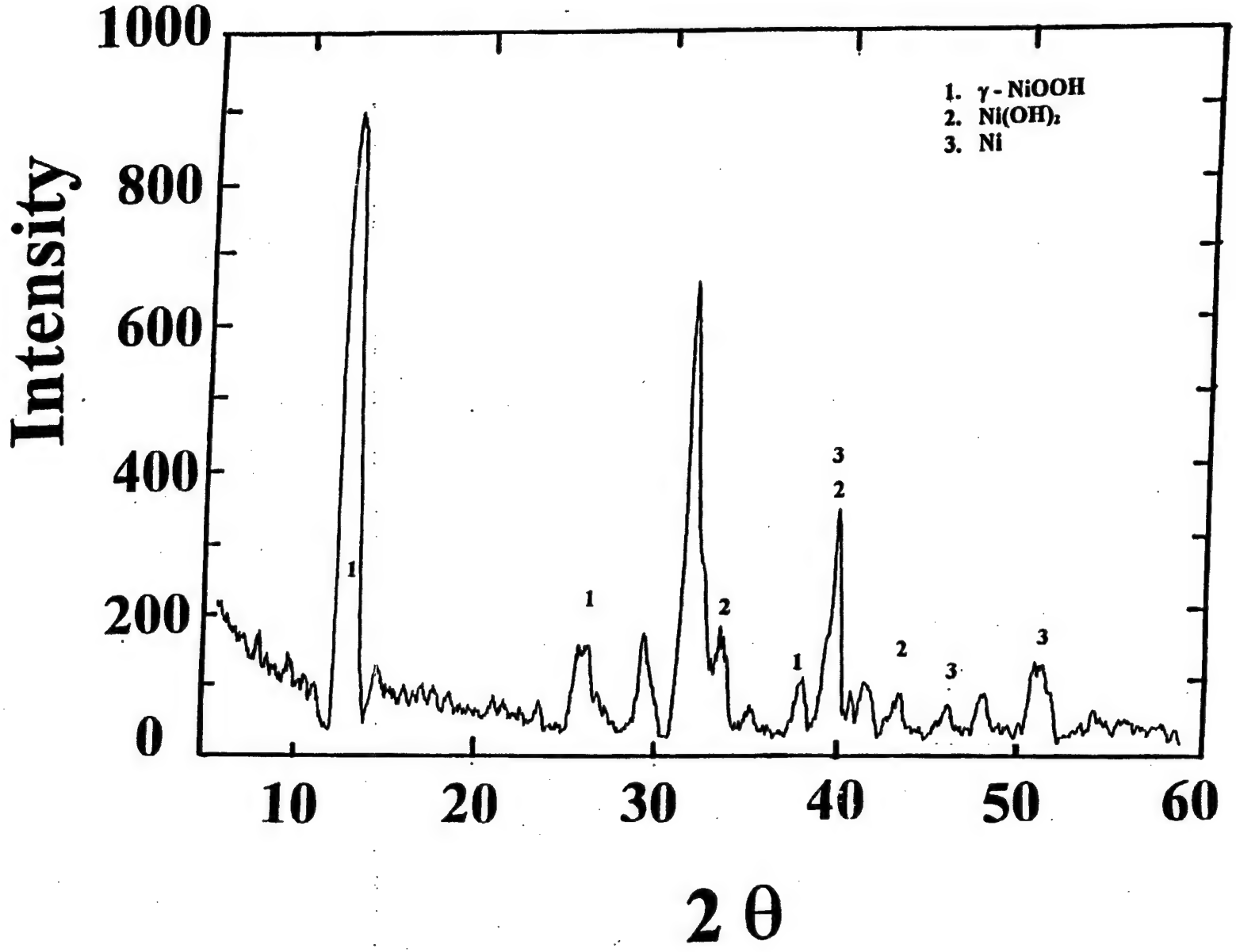

Figure 30. In-situ x-ray diffraction pattern obtained for 12.5 µm (0.0005") thick nickel foil mounted on the electrochemical test cell filled with KOH, after exposure for 24 hours at - 800 mV versus a Ni/NiO electrode.

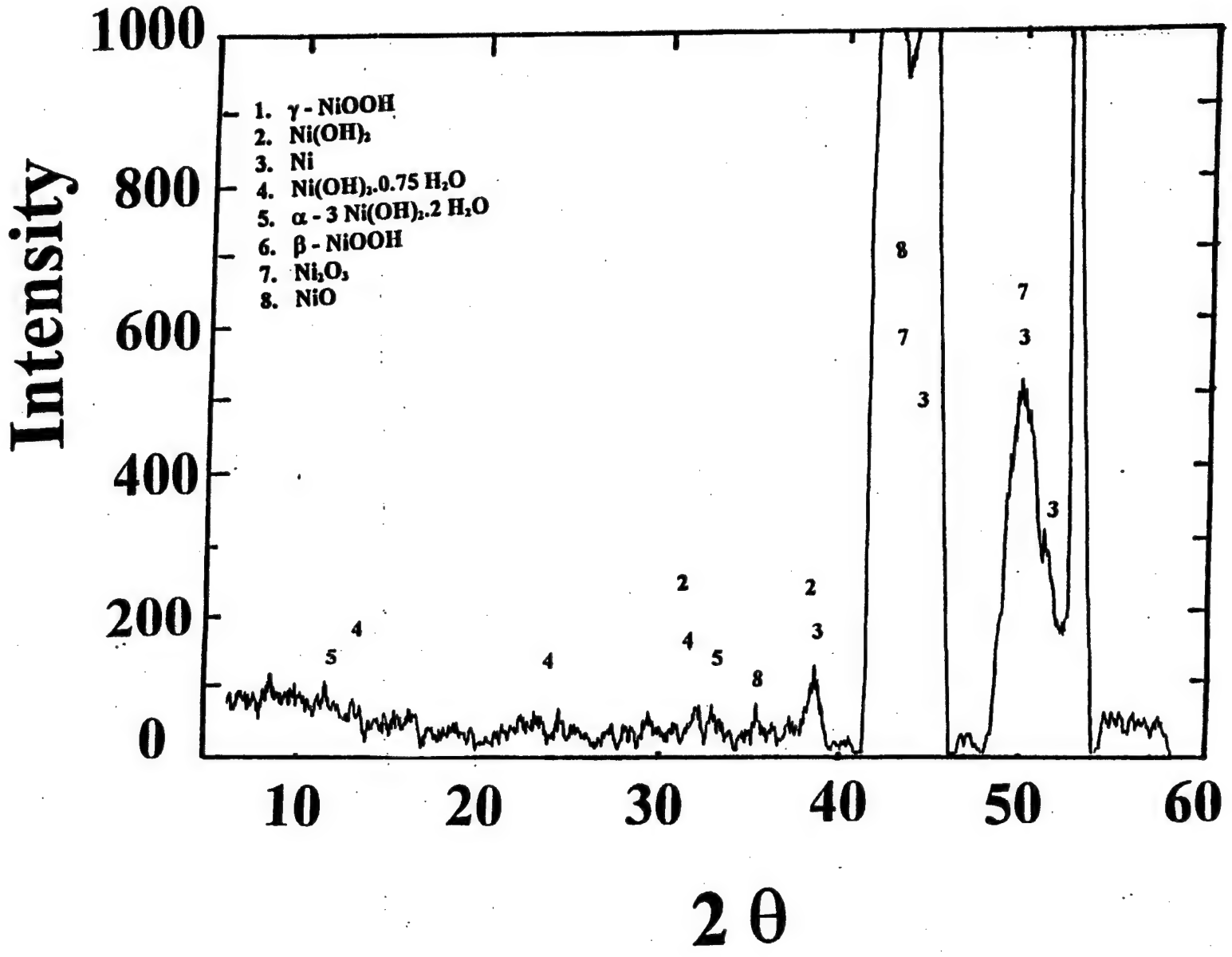

Figure 31. In-situ x-ray diffraction pattern obtained for 12.5 μm (0.0005") thick nickel foil mounted on the electrochemical test cell filled with KOH, after exposure for 0.5 hour at + 450 mV versus a Ni/NiO electrode.

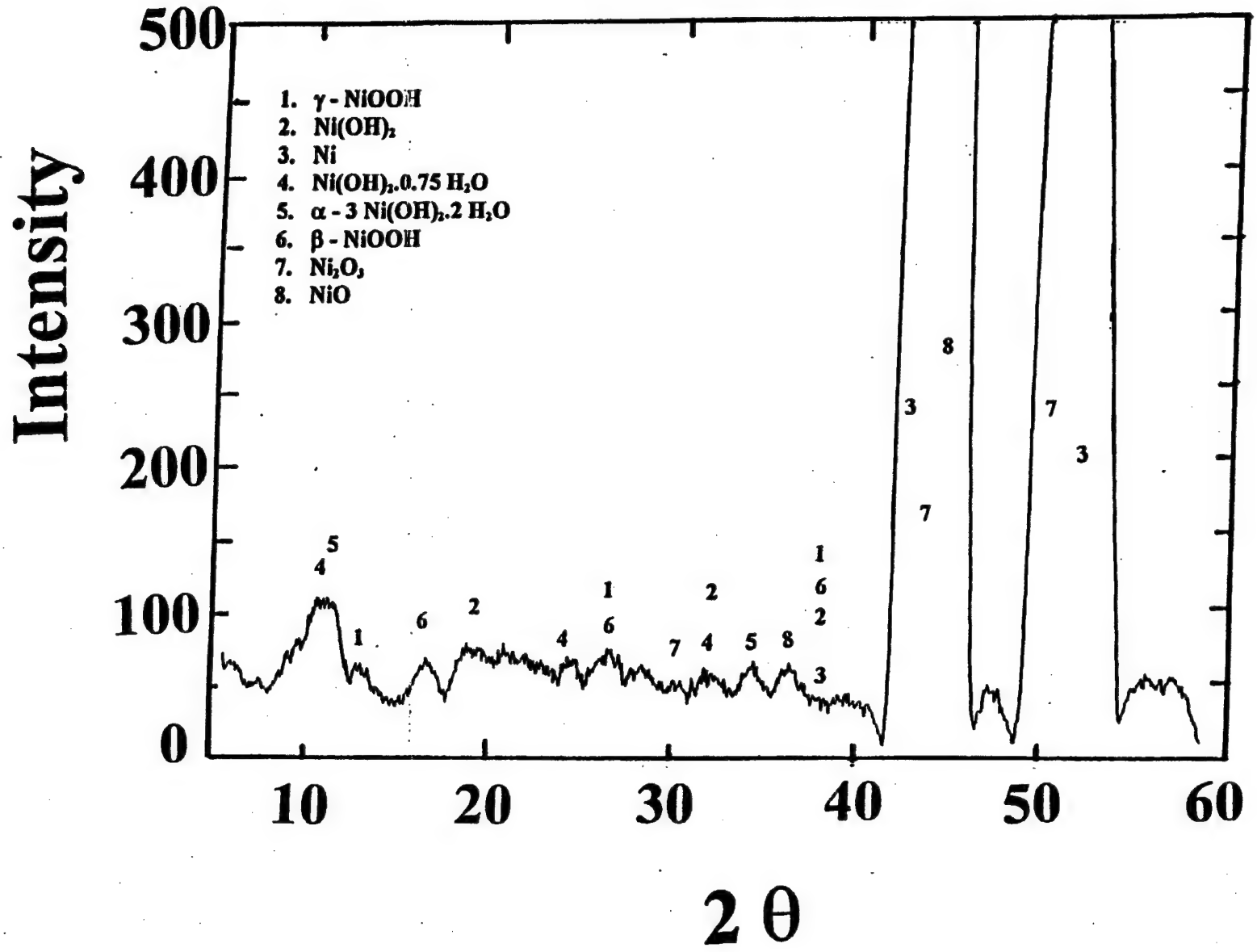

Figure 32. In-situ x-ray diffraction pattern obtained for 12.5 μm (0.0005") thick nickel foil mounted on the electrochemical test cell filled with KOH, after exposure for 1 hours at + 450 mV versus a Ni/NiO electrode.

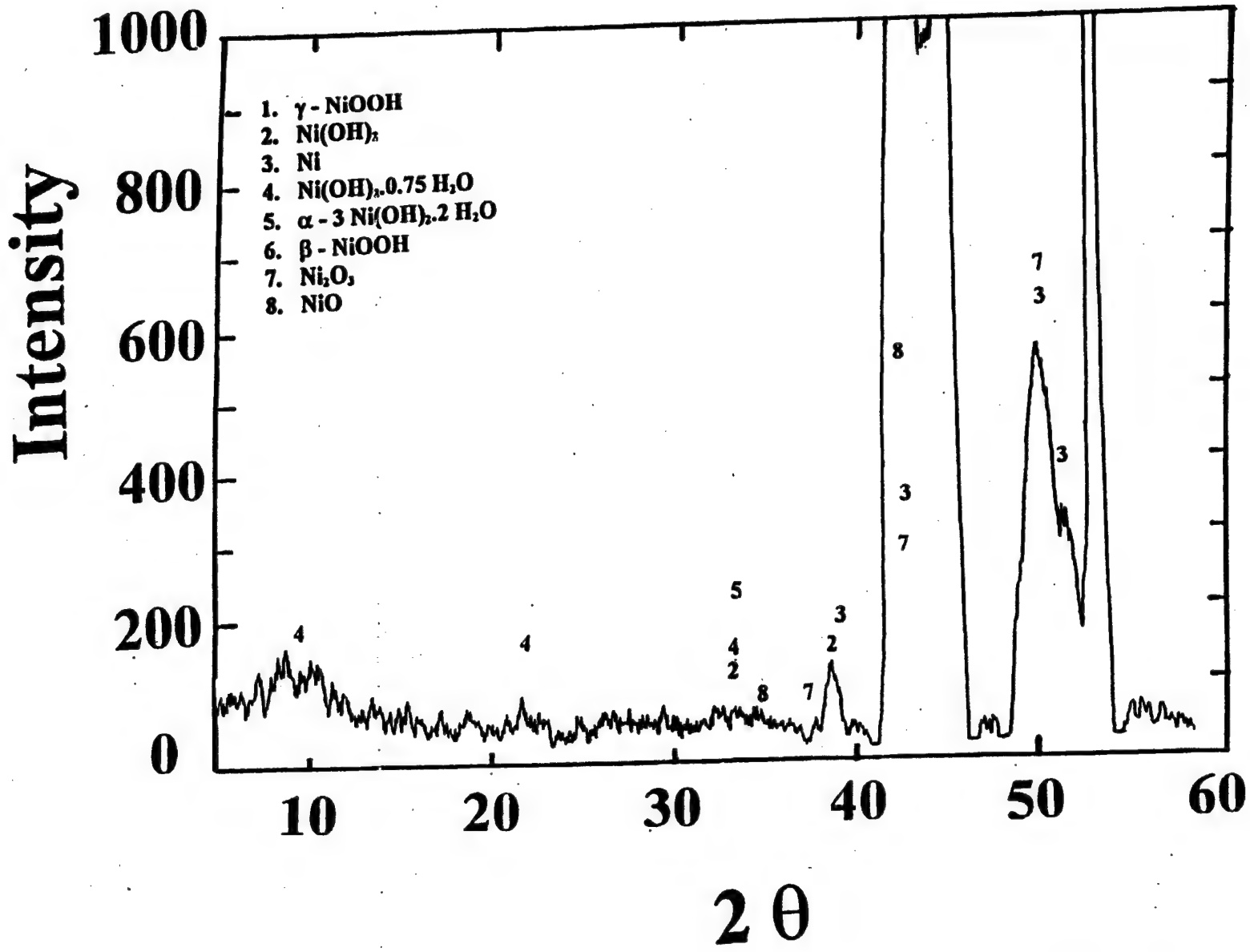

Figure 33. In-situ x-ray diffraction pattern obtained for 12.5 μm (0.0005") thick nickel foil mounted on the electrochemical test cell filled with KOH, after exposure for 3 hours at + 450 mV versus a Ni/NiO electrode.

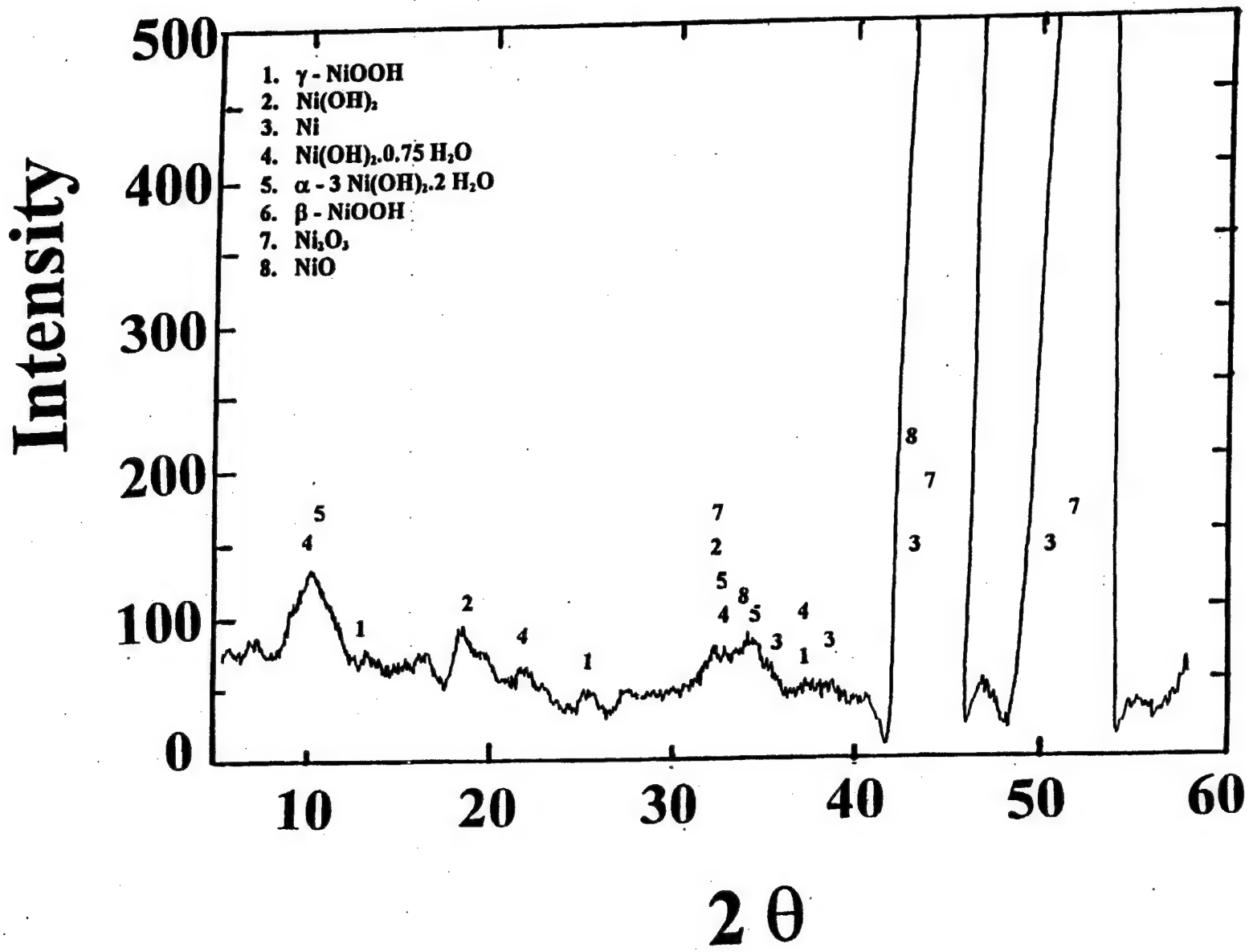

Figure 34. In-situ x-ray diffraction pattern obtained for 12.5 μm (0.0005") thick nickel foil mounted on the electrochemical test cell filled with KOH, after exposure for 2.4 hours at + 450 mV versus a Ni/NiO electrode.

foil. The remaining γ - NiOOH layers oxidize to form NiO and or Ni_2O_3. The progression of the chemical reaction can be represented as follows.

$$Ni \Rightarrow Ni(OH)_2 \Rightarrow Ni(OH)_2 .0.75\ H_2O \Rightarrow 3Ni(OH)_2 .2\ H_2O$$

$$\Rightarrow Ni^{+3}OOH \Rightarrow Ni^{+3}{}_2O_3 \Rightarrow Ni^{+2}O$$

$$Ni^{+3}OOH \Rightarrow Ni^{+3}{}_2O_3 \Rightarrow Ni^{+2}O$$

The present investigation leads us to a conclusion that the nickel surface layers are oxidized following the contact with alkaline solution (KOH and / or sea water). The oxide film instead of passivating the surface layers tend to migrate into the bulk of metal during the electrochemical process. The chemical transformation of oxide layer depends upon the applied potential. While reduction occurs at – 800 mV, the oxide layer undergoes further oxidation at + 450 mV.

CONCLUSIONS

1. The experimental technique that has been described here can successfully determine the structure of the passive layer at the metal - solution interface during an electrochemical process.
2. During the electrochemical reaction of the nickel/sea water system, at - 800 mV, significant $Ni(OH)_2$ and γ - NiOOH are formed at the interface. From XRD and XPS analysis of the structure of the interface, it is possible to suggest that $Ni(OH)_2$ is present at the outer passive layer and γ - NiOOH is present at the inner passive layer.

3. At + 450 mV the interface (inner and outer passive layers) structure consists of NiO, Ni_2O_3, $Ni(OH)_2$ and γ - NiOOH. The inner passive layer is comprised of γ - NiOOH, and the outer passive layer is comprised of Ni_2O_3 and $Ni(OH)_2$.

ACKNOWLEDGEMENT

The author acknowledges the usage of the x-ray diffraction unit purchased by the Geology Department of the George Washington University under an NSF grant to Prof. Fred Siegel. The author would like to thank Prof. C. Gilmore of the Institute of Materials Science, George Washington University for permitting us to conduct experiments in his thin film laboratory. The author thanks Mr. Paul Goldy of the thin film laboratory of the Institute of Materials Science, George Washington University for his help in conducting experiments with the x-ray diffraction unit and for the operation of the XPS unit.

REFERENCES

1. Ross, P. N., and Wagner, F. T., "The Application of Surface Physics Techniques to the Study of Electrochemical Systems," Advances in Electrochem., 13, 69(1985).

2. Flischmann, M. and Hill, I. R., "Surface Enhanced Raman Spectroscopy," edt. Chang, R. K. and Furtak, T. 5., Plenum Pub., New York, 275 (1982).

3 Bewick, A. and Pons, B. S., "Advances in Infra-red and Raman Spectroscopy," edt. Clark, R. J. H., and Hester, RE., Pub., Wiley Heydon, New York 12, Chap. 1(1985).

4. Bomchil, O., and Rekel, C., " Neutron Diffraction Study of the Electrochemical Passivation of Nickel Powder," Electro Anal. Chem., 101, 133(1979).

5. Lang, G. G., Kruger, J., Black, D. R. and Kuriyama, M., "Structure of Passive Films on Iron Using a New Surface–EXAFS Technique," J. Electrochem. Soc., 130, 240 (1983).

6. Bosio, L., Cones, R. and Froment, M., "Reflection EXAFS Studies of Protective Oxide Formation on Metal Surfaces," Proc. 3rd Int. EXAFS Conf., Stanford, CA (1984).

7. Marra, W. C., Elsenberger, P. and Cho, A. Y., J., " x-ray Total – External – Reflection – Bragg Diffraction: A Structural Study of Gallium Arsenide – Aluminum Interface," Appl. Phys, 50, 6927(1979).

8. Cowan, P. L., Goloychenko, J. A. and Robbins, M.F., " x- ray Standing Waves at the Crystal Surface," Phys. Rev. Lett., 44, 1680 (1980).

9. Golovchenko, J. A., Patel, S. W, Kaplan, D. R., Cowan, P. L., and Bedzyk, P., "Solution to the Surface Registration Problem Using x- Ray Standing Waves," Phys. Rev. Lett., 49, 560(1982).

10 A. Srinivasa Rao and J. N. Murray., "Characterization of Surface Film Growth During the Electrochemical Process : Part I," NSWC CD –TR–61-98–17, June 1998.

11. A. Srinivasa Rao "Characterization of Surface Film Growth During the Electrochemical Process : Part II (90% Copper – 10 % Nickel System)," NSWC CD –TR–61-98– 21, Sept. 1998.

12. A. Srinivasa Rao "Characterization of Surface Film Growth During the Electrochemical Process : Part III (70% Copper – 30 % Nickel System)," NSWC CD –TR–61-98– 24, Oct. 1998.

13. Pandya, K. I., O'Grady, W. E.Corrigan, D. A., Mc Breen, J. and Hoffman, R. W., " In – situ x – Ray Adsorption Spectroscopic Studies of Nickel Oxide Electrodes," J. Phys. Chem, 94, 21(1990)).

14. Rommel, H. E.G., "Time Dependent Energy Efficiency Losses at Nickel Cathodes in Alkaline Water Electrolysis Systems," MS Thesis, Johns Hopkins University, Baltimore, MD 1982.

15. Moran, P. J., and Guanti, R. S., "Measurement of Electrolyte Conductivity in Highly Conducting Solutions," 161st Electrochem. Soc., Meeting, Montreal, Canada, 1982.

16. Wagner, C. D., Riggs, W. M., Davis, L. E., Moulder, J. F. and Muilenberg, G. E., "Handbook of X-Ray Photoelectron Spectroscopy," Pub. By Perkin-Elmer Corp., Eden Prairie, MN (1979).

DISTRIBUTION

Copies		Copies	Center Distribution	
1	DTIC			
		1	60	(Morton)
		1	61	(Holsberg)
		1	612	(Aprigliano)
		1	613	(Ferrara)
		1	614	(Montemarano)
		1	615	(DeNale)
		1	0113	(Douglas)
		5	612	(Rao)